Ionosphere-Thermosphere Coupling

Shigeto Watanabe
Hokkaido University

Solar Radiation

HINODE/XRT
(0.6nm～20nm)

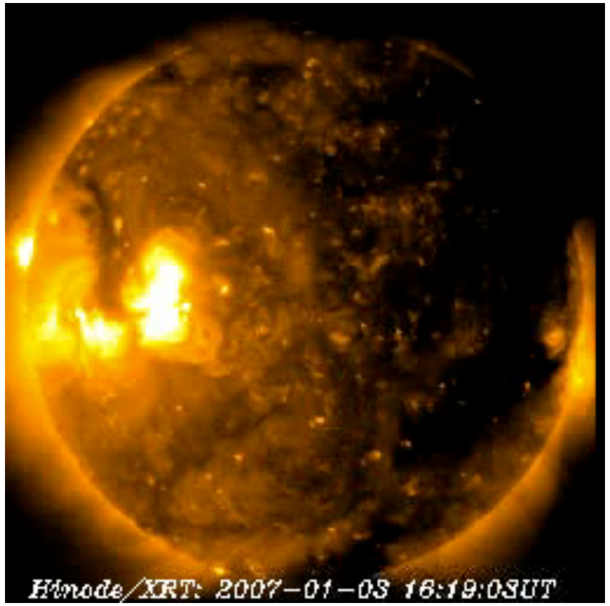

EUV: Extreme UltraViolet

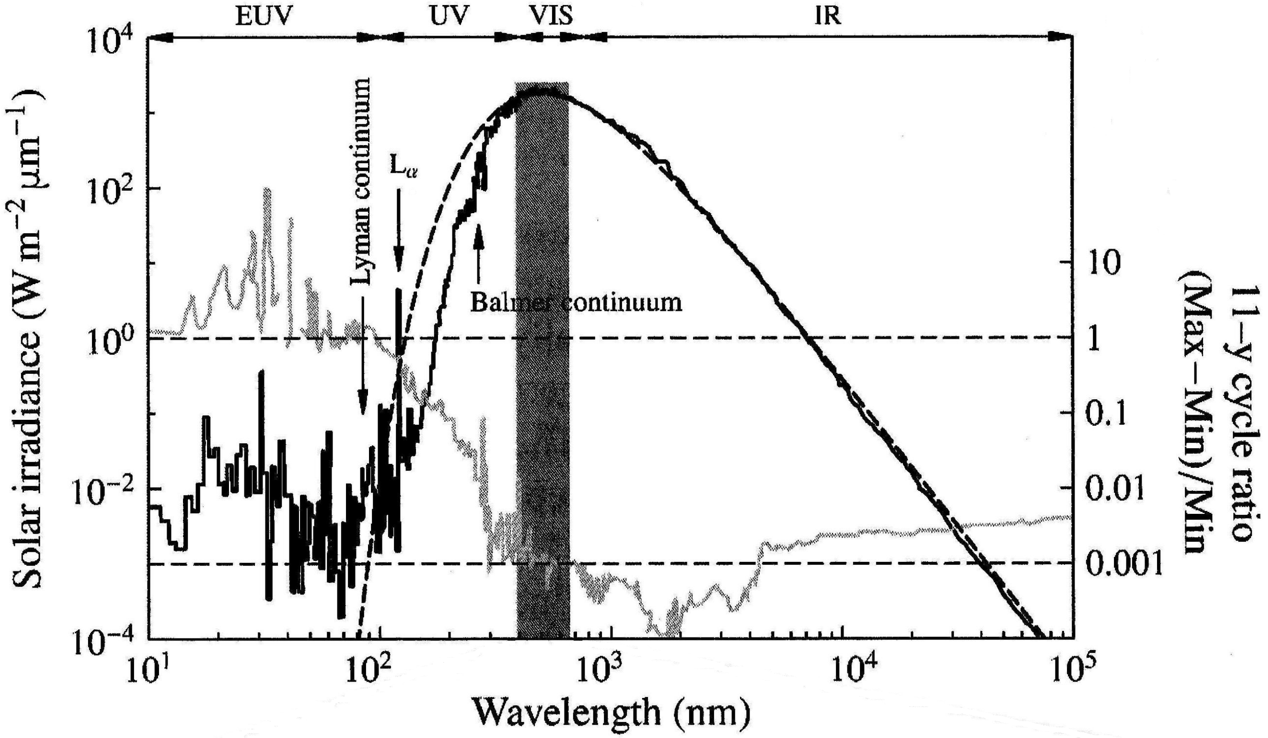

Planck's law $$I(\lambda)=\frac{2hc^2}{\lambda^5}\frac{1}{e^{\frac{hc}{k\lambda T}}-1}$$

Stefan–Boltzmann law $$F=\int_0^\infty I(\lambda)d\lambda=\sigma T^4$$

$$C_s=1.37\mathrm{kW/m^2}$$

Solar Constant

Photochemistry in the Upper Atmosphere

Photoionization by EUV

$$O + hv \rightarrow O^+ + e$$

$$O_2 + hv \rightarrow O_2^+ + e$$

$$N_2 + hv \rightarrow N_2^+ + e$$

$$He + hv \rightarrow He^+ + e$$

Radiative Recombination

$$O^+ + e \rightarrow O + hv$$

$$He^+ + e \rightarrow He + hv$$

$$H^+ + e \rightarrow H + hv$$

Electron-Ion Recombination

$$NO^+ + e \rightarrow N + O$$

$$O_2^+ + e \rightarrow O + O$$

$$N_2^+ + e \rightarrow N + N$$

Ion-Molecule Reactions

$$O^+ + N_2 \rightarrow NO^+ + N$$

$$O^+ + O_2 \rightarrow O + O_2^+$$

$$O_2^+ + NO \rightarrow O_2 + NO^+$$

$$N_2^+ + O \rightarrow NO^+ + N$$

$$N_2^+ + O_2 \rightarrow N_2 + O_2^+$$

$$H^+ + O \rightarrow H + O^+$$

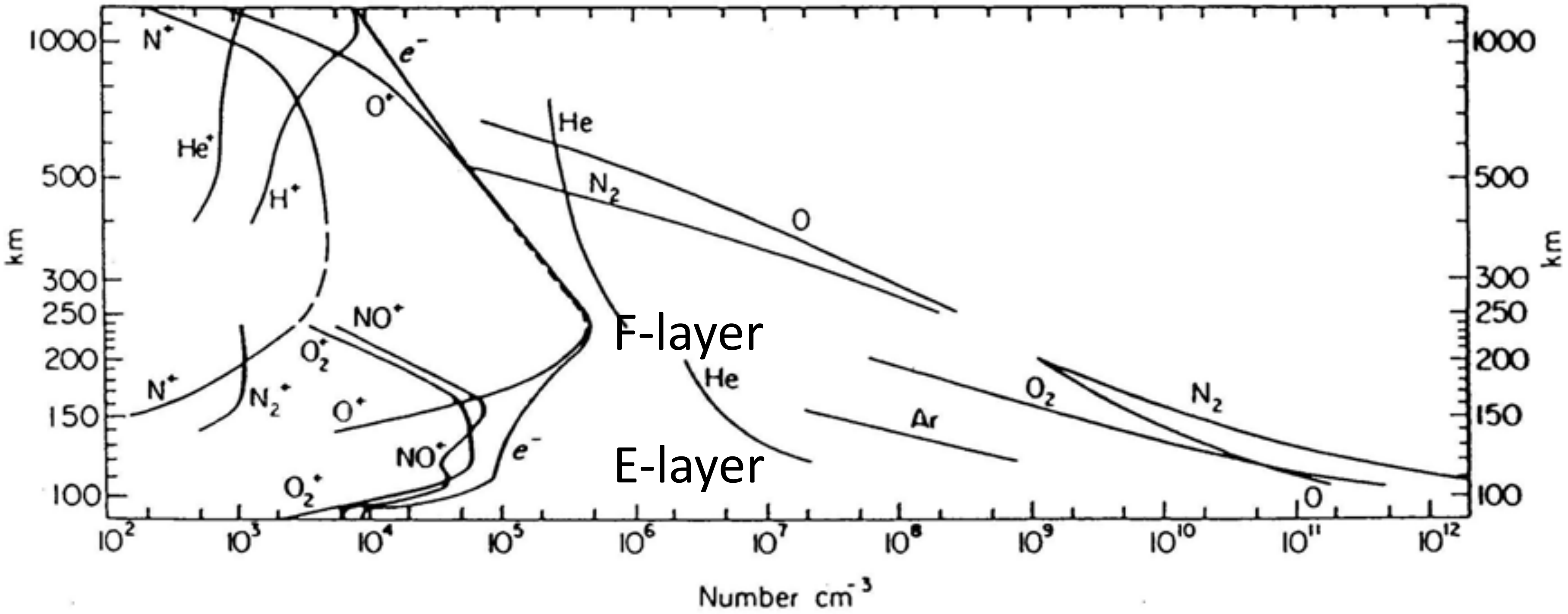

Ionosphere Thermosphere

*Ionization rate is $<10^{-4}$ in F-region.

*Coupling between Atmosphere and Plasma is important for the dynamics and photochemistry in the ionosphere/thermosphere.

Lorentz force $\mathbf{F} = q\left(\mathbf{E} + \mathbf{v} \times \mathbf{B}\right)$

Momentum equation $m\frac{d\mathbf{v}}{dt} = q\left(\mathbf{E} + \mathbf{v} \times \mathbf{B}\right)$

when $\mathbf{E} = 0$

$$m\frac{d\mathbf{v}}{dt} = q\left(\mathbf{v} \times \mathbf{B}\right)$$

$$m\mathbf{v}\frac{d\mathbf{v}}{dt} = q\mathbf{v}\left(\mathbf{v} \times \mathbf{B}\right)$$

$$\frac{d}{dt}\left(\frac{m\mathbf{v}^2}{2}\right) = 0$$

$$\frac{d^2\mathbf{v}_\perp}{dt^2} = -\left(\frac{qB}{m}\right)^2 \mathbf{v}_\perp$$

Cycrotron frequency $\omega = \frac{qB}{m}$, $r_L = \frac{\mathrm{v}}{\omega}$ **Larmor radius**

$$\frac{d\mathbf{v}_{//}}{dt} = 0$$

Drift Motion of Charged Particle

$$\mathbf{v}(\mathbf{r},t) = \mathbf{v}_c(\mathbf{r},t) + \mathbf{v}_d(\mathbf{r})$$

$\mathbf{v}_c$ Velocity of Cyclotron Motion $\mathbf{v}_d$ Drift Motion perpendicular to the Local Magnetic Field Line

$$m\frac{d\mathbf{v}_c}{dt} = q\mathbf{E} + q(\mathbf{v}_c \times \mathbf{B}) + q(\mathbf{v}_d \times \mathbf{B})$$

In the $\mathbf{v}_d = \dfrac{\mathbf{E}\times\mathbf{B}}{B^2}$ Frame, $m\dfrac{d\mathbf{v}_c}{dt} = q(\mathbf{v}_c \times \mathbf{B})$ Cyclotron Motion

When the force to the Charged Particle is $\mathbf{f}$

$$\mathbf{v}_d = \frac{\mathbf{f}\times\mathbf{B}}{qB^2}$$

Drift Directions are different for Ions and Electrons

→ Generation of Currents → Generation of Magnetic Field

Momentum Equations

$$\rho_e \frac{\partial \mathbf{v}_e}{\partial t} + \rho_e(\mathbf{v}_e \cdot \nabla)\mathbf{v}_e = -\nabla p_e - \frac{e\rho_e}{m_e}(\mathbf{E} + \mathbf{v}_e \times \mathbf{B}) - \rho_e \nu_{ei}(\mathbf{v}_e - \mathbf{v}_i)$$

$$\rho_i \frac{\partial \mathbf{v}_i}{\partial t} + \rho_i(\mathbf{v}_i \cdot \nabla)\mathbf{v}_i = -\nabla p_i + \frac{e\rho_i}{m_i}(\mathbf{E} + \mathbf{v}_i \times \mathbf{B}) - \rho_i \nu_{ie}(\mathbf{v}_i - \mathbf{v}_e)$$

If

$m_e << m_i$, $|n_i - n_e| << n_i, n_e$ **: Quasi Neutrality** $(n_i \approx n_e)$

Ambipolar Electric Field

$$\mathbf{E} = -\frac{\nabla p_e}{e n_e}, \qquad -\nabla \phi = -\frac{\nabla p_e}{e n_e}, \qquad \phi = \frac{kT_e}{e}$$

Ions and Electrons as Fluid are moving together.

$$\therefore \rho \frac{\partial \mathbf{V}}{\partial t} + \rho(\mathbf{V} \cdot \nabla)\mathbf{V} = -\nabla p + (\mathbf{J} \times \mathbf{B}), \qquad p = p_i + p_e$$

Momentum Equations of Ions and Electrons along Local Magnetic Field Lines for Frequent Collisions

$$-\nabla p_{i//} + nm_i\mathbf{g}_{//} + ne\mathbf{E}_{//} - nm_i\nu_{in}\left(\mathbf{v}_{i//} - \mathbf{u}_{n//}\right) = 0$$

$$-\nabla p_{e//} + nm_e\mathbf{g}_{//} - ne\mathbf{E}_{//} - nm_e\nu_{en}\left(\mathbf{v}_{e//} - \mathbf{u}_{n//}\right) = 0$$

$$\begin{pmatrix} n_i \approx n_e \\ \mathbf{v}_{i//} \approx \mathbf{v}_{e//} \end{pmatrix}$$ Charge Neutrality

$$\mathbf{v}_{//} = \mathbf{u}_{n//} - D\left(\frac{\partial p}{p\partial s} - \frac{1}{H_{//}}\right)$$

Continuity Equation $\frac{\partial n}{\partial t} = q - L - \frac{\partial n\mathbf{v}_{//}}{\partial s}$

$$p = nk\left(T_i + T_e\right), \qquad H_{//} = \frac{k\left(T_i + T_e\right)}{m_i g_{//}}, \qquad D = \frac{k\left(T_i + T_e\right)}{m_i \nu_{in}}$$

Momentum Equations of Ions and Electrons perpendicular to Local Magnetic Field Lines for Frequent Collisions

$$-\nabla p_{i\perp} + nm_i\mathbf{g}_\perp + ne\left(\mathbf{E}_\perp + \mathbf{v}_{i\perp}\times\mathbf{B}\right) - nm_i\nu_{in}\left(\mathbf{v}_{i\perp} - \mathbf{u}_{n\perp}\right) = 0$$

$$-\nabla p_{e\perp} + nm_e\mathbf{g}_\perp - ne\left(\mathbf{E}_\perp + \mathbf{v}_{e\perp}\times\mathbf{B}\right) - nm_e\nu_{en}\left(\mathbf{v}_{e\perp} - \mathbf{u}_{n\perp}\right) = 0$$

Current Conservation $\nabla\mathbf{J} = \nabla\left(en_i\mathbf{v}_i - en_e\mathbf{v}_e\right) = 0$

Charge Neutrality $n_i \approx n_e$

then, $\mathbf{v}_i \approx \mathbf{v}_e$

in detail

$$\mathbf{v}_i = \frac{\nu_{in}\Omega_i}{\nu_{in}^2+\Omega_i^2}\left(\frac{\mathbf{E}}{B} - \frac{\nabla p_i}{nm_i\Omega_i} + \frac{\mathbf{g}}{\Omega_i} + \frac{\nu_{in}\mathbf{u}_n}{\Omega_i}\right) + \frac{\Omega_i^2}{\nu_{in}^2+\Omega_i^2}\left(\frac{\mathbf{E}}{B} - \frac{\nabla p_i}{nm_i\Omega_i} + \frac{\mathbf{g}}{\Omega_i} + \frac{\nu_{in}\mathbf{u}_n}{\Omega_i}\right)\times\frac{\mathbf{B}}{B}$$

$$\mathbf{v}_e = -\frac{\nu_{en}\Omega_e}{\nu_{en}^2+\Omega_e^2}\left(\frac{\mathbf{E}}{B} + \frac{\nabla p_e}{nm_e\Omega_e} - \frac{\mathbf{g}}{\Omega_e} - \frac{\nu_{en}\mathbf{u}_n}{\Omega_e}\right) + \frac{\Omega_e^2}{\nu_{en}^2+\Omega_e^2}\left(\frac{\mathbf{E}}{B} + \frac{\nabla p_e}{nm_e\Omega_e} - \frac{\mathbf{g}}{\Omega_e} - \frac{\nu_{en}\mathbf{u}_n}{\Omega_e}\right)\times\frac{\mathbf{B}}{B}$$

Collision Frequency between Ion and Neutral Particle

$$\nu_{in} = 2.6\times10^{-9}(n_n + n_i)M_n^{-0.5}$$

M_n : average atomic mass of neutral particles

Collision Frequency of Electron

$$\nu_e = \nu_{en} + \nu_{ei}$$
$$= 5.4\times10^{-10} n_n T_e^{0.5} + \left(34 + 4.18\ln\left(T_e^3 / n_e\right)\right) n_e T_e^{-1.5}$$

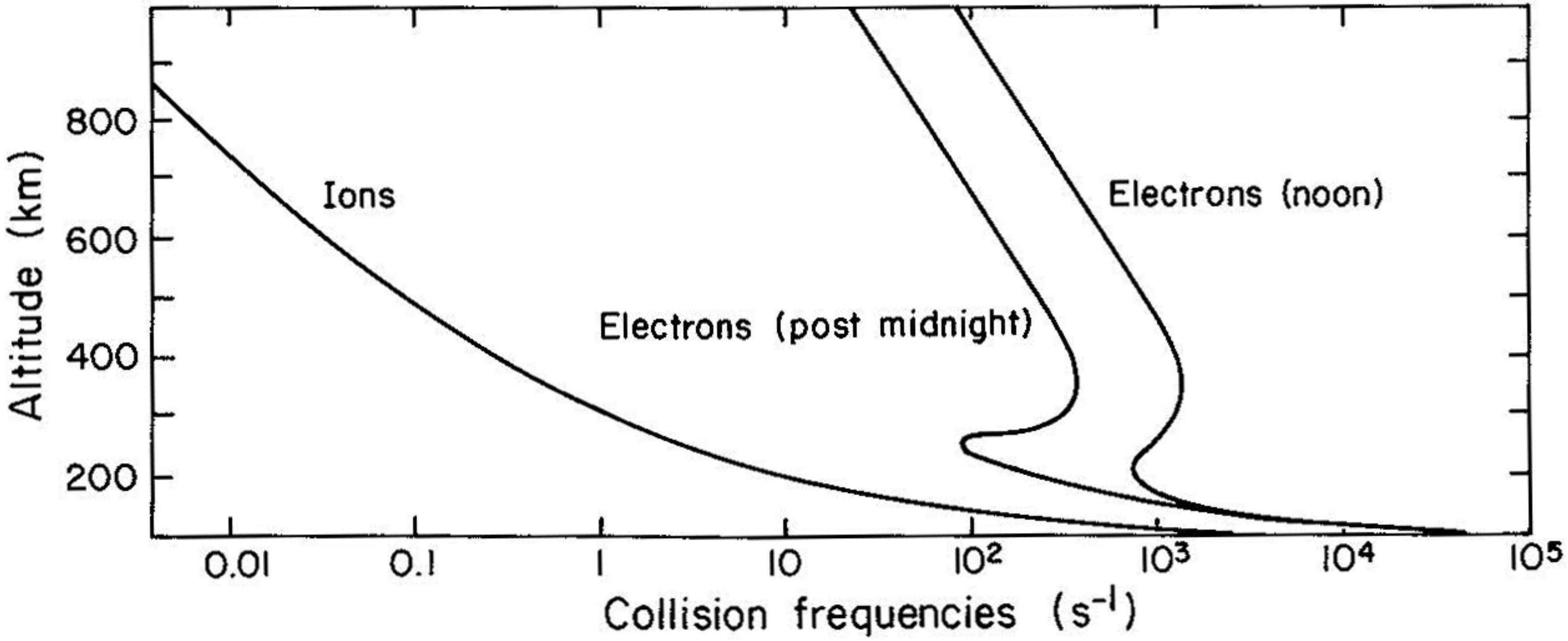

$$\mathbf{J} = en\left(\mathbf{V}_i - \mathbf{V}_e\right)$$

$$\Omega_i >> \nu_{in}, \qquad \Omega_e >> \nu_{en} \qquad \mathbf{J} \approx en\left(-\frac{\nabla p_i}{nm_i\Omega_i} - \frac{\nabla p_e}{nm_e\Omega_e} + \frac{\mathbf{g}}{\Omega_i}\right) \times \frac{\mathbf{B}}{B} \approx 0$$

$$\left[\frac{\nabla p}{nm\Omega} \approx \frac{nkT}{nm\Omega H} \approx V_{th}\,\frac{r_L}{H}\right]$$

$$\Omega_i < \nu_{in}, \qquad \Omega_e >> \nu_{en} \qquad \mathbf{J} \approx en\left(\mathbf{u}_n - \frac{\mathbf{E}\times\mathbf{B}}{B^2}\right)$$

$$\Omega_i < \nu_{in}, \qquad \Omega_e < \nu_{en} \qquad \mathbf{J} \approx 0$$

Current Layer (Dynamo Region)

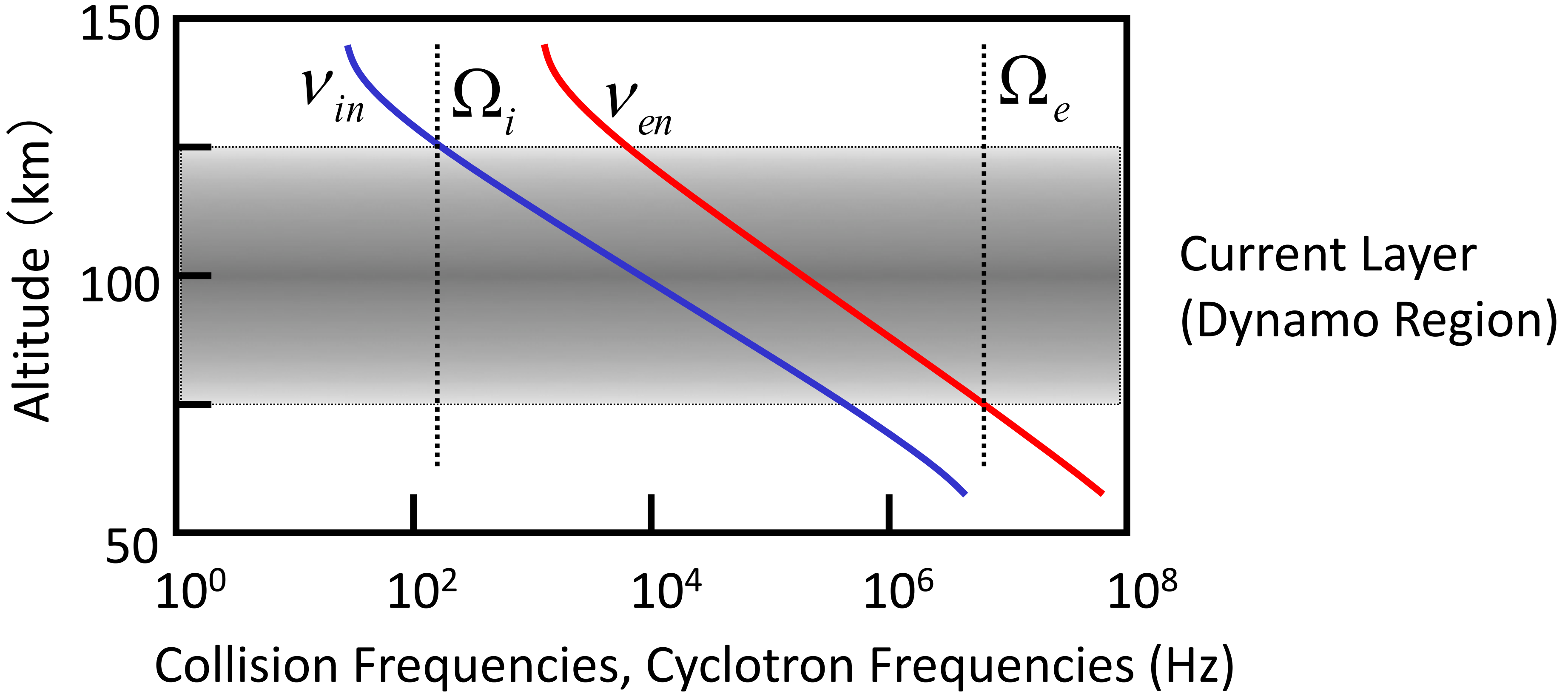

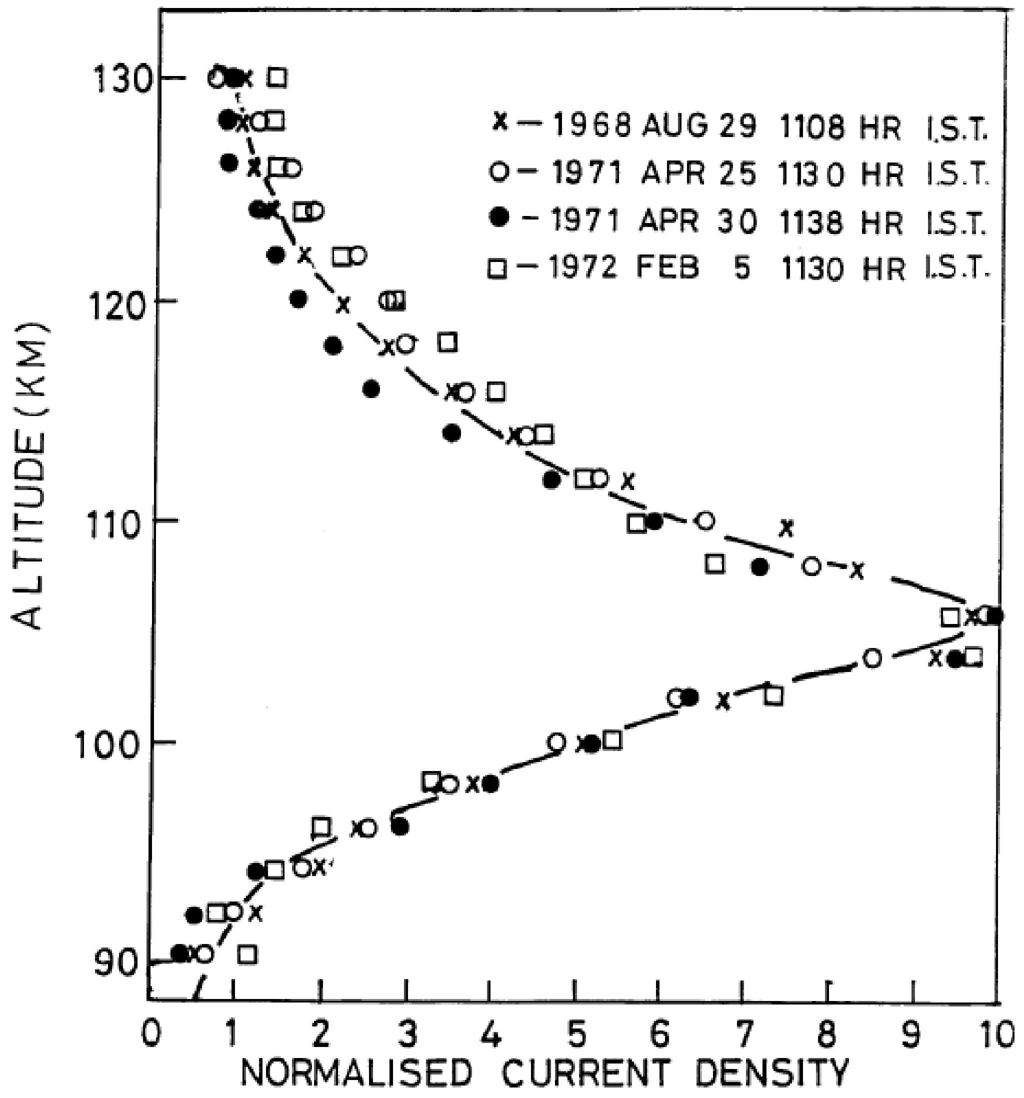

Fig. 6. The vertical distribution of the equatorial electrojet current density measured during four midday flights from Thumba, plotted after normalizing the peak current densities to 10 Amp. km^{-2}. The full line shows the average distribution (after Sampath and Sastry, 1979a).

$$\mathbf{J} = en(\mathbf{v}_i - \mathbf{v}_e)$$

$$\mathbf{v}_{i\perp} = \frac{\nu_{in}\Omega_i}{\nu_{in}^2 + \Omega_i^2}\frac{\mathbf{E}_\perp}{B} + \frac{\Omega_i^2}{\nu_{in}^2 + \Omega_i^2}\frac{\mathbf{E}_\perp \times \mathbf{B}}{B^2}$$

$$\mathbf{v}_{e\perp} = -\frac{\nu_{en}\Omega_e}{\nu_{en}^2 + \Omega_e^2}\frac{\mathbf{E}_\perp}{B} + \frac{\Omega_e^2}{\nu_{en}^2 + \Omega_e^2}\frac{\mathbf{E}_\perp \times \mathbf{B}}{B^2}$$

$$\mathbf{v}_{i//} = \frac{e}{m_i \nu_{in}}\mathbf{E}_{//}$$

$$\mathbf{v}_{e//} = -\frac{e}{m_e \nu_{en}}\mathbf{E}_{//}$$

$$\mathbf{J} = en\left\{\left(\frac{\nu_{in}\Omega_i}{\nu_{in}^2 + \Omega_i^2} + \frac{\nu_{en}\Omega_e}{\nu_{en}^2 + \Omega_e^2}\right)\frac{\mathbf{E}_\perp}{B} + \left(\frac{\Omega_i^2}{\nu_{in}^2 + \Omega_i^2} - \frac{\Omega_e^2}{\nu_{en}^2 + \Omega_e^2}\right)\frac{\mathbf{E}_\perp \times \mathbf{B}}{B^2} + \left(\frac{e}{m_i \nu_{in}} + \frac{e}{m_e \nu_{en}}\right)\mathbf{E}_{//}\right\}$$

$$\mathbf{J} = \sigma_P \mathbf{E}_\perp + \sigma_H \mathbf{E}_\perp \times \mathbf{B} / B + \sigma_{//}\mathbf{E}_{//}$$

Conductivity

$$\sigma_P = \frac{en}{B}\left(\frac{\nu_{in}\Omega_i}{\nu_{in}^2 + \Omega_i^2} + \frac{\nu_{en}\Omega_e}{\nu_{en}^2 + \Omega_e^2}\right)$$ Pedersen

$$\sigma_H = \frac{en}{B}\left(\frac{\Omega_i^2}{\nu_{in}^2 + \Omega_i^2} - \frac{\Omega_e^2}{\nu_{en}^2 + \Omega_e^2}\right)$$ Hall

$$\sigma_{//} = \frac{en}{B}\left(\frac{\Omega_i}{\nu_{in}} + \frac{\Omega_e}{\nu_{en}}\right)$$ Longitudinal

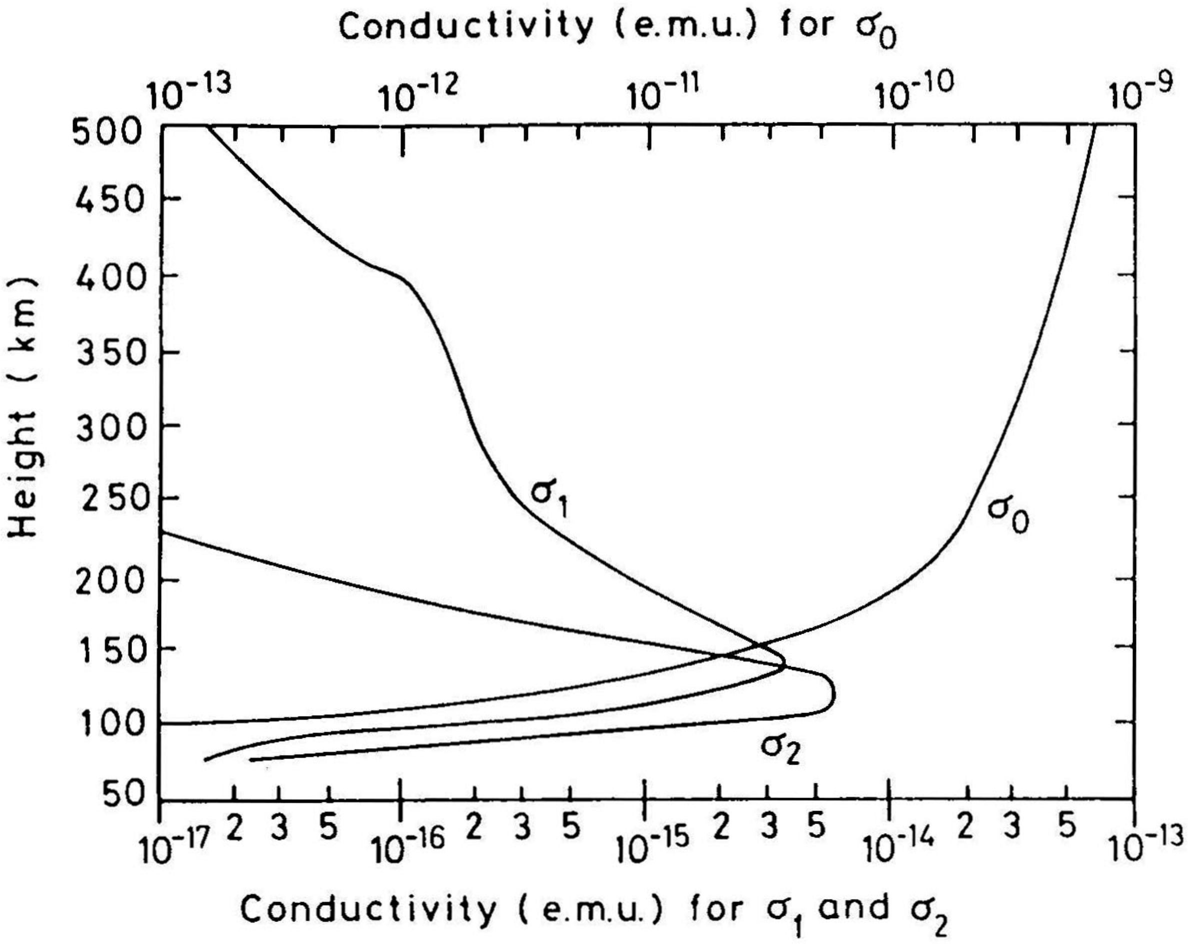

Fig. 6.23 Conductivity profiles calculated for middle latitude at noon. (S.-I. Akasofu and S. Chapman (after K. Maeda and H. Matsumoto), *Solar–Terrestrial Physics*. Oxford University Press, 1972. By permission of Oxford University Press)

E-Region Dynamo

$$\mathbf{J} \approx en\left(\mathbf{u}_n - \frac{\mathbf{E}\times\mathbf{B}}{B^2}\right)$$

$$\nabla\cdot\mathbf{J} = \nabla\cdot\left(en\left(\mathbf{u}_n - \frac{\mathbf{E}\times\mathbf{B}}{B^2}\right)\right) = 0$$

$$\therefore \mathbf{E} = -\mathbf{u}_n \times \mathbf{B}$$

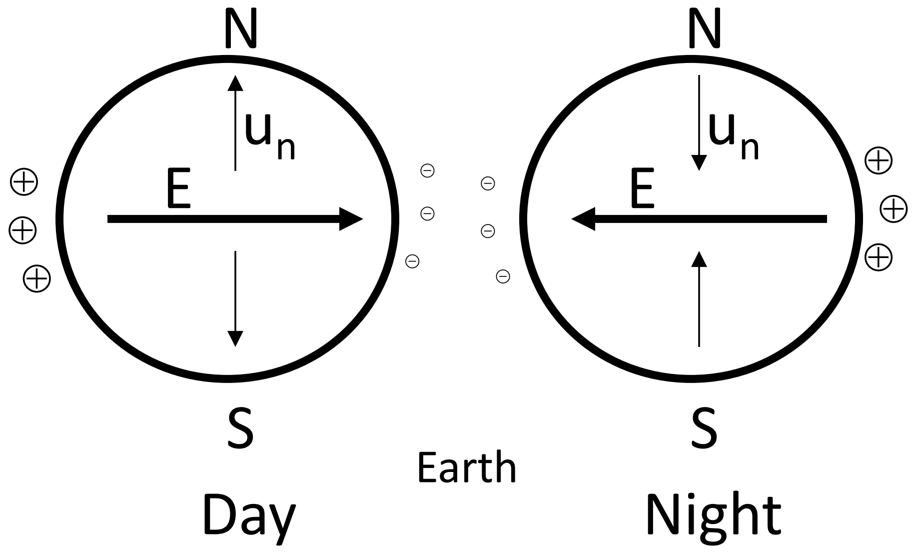

Sq (Solar quiet) currents

L current (Lunar current)
DP-1 current (auroral electrojets)
DP-2 current (two cell current within polar cup)

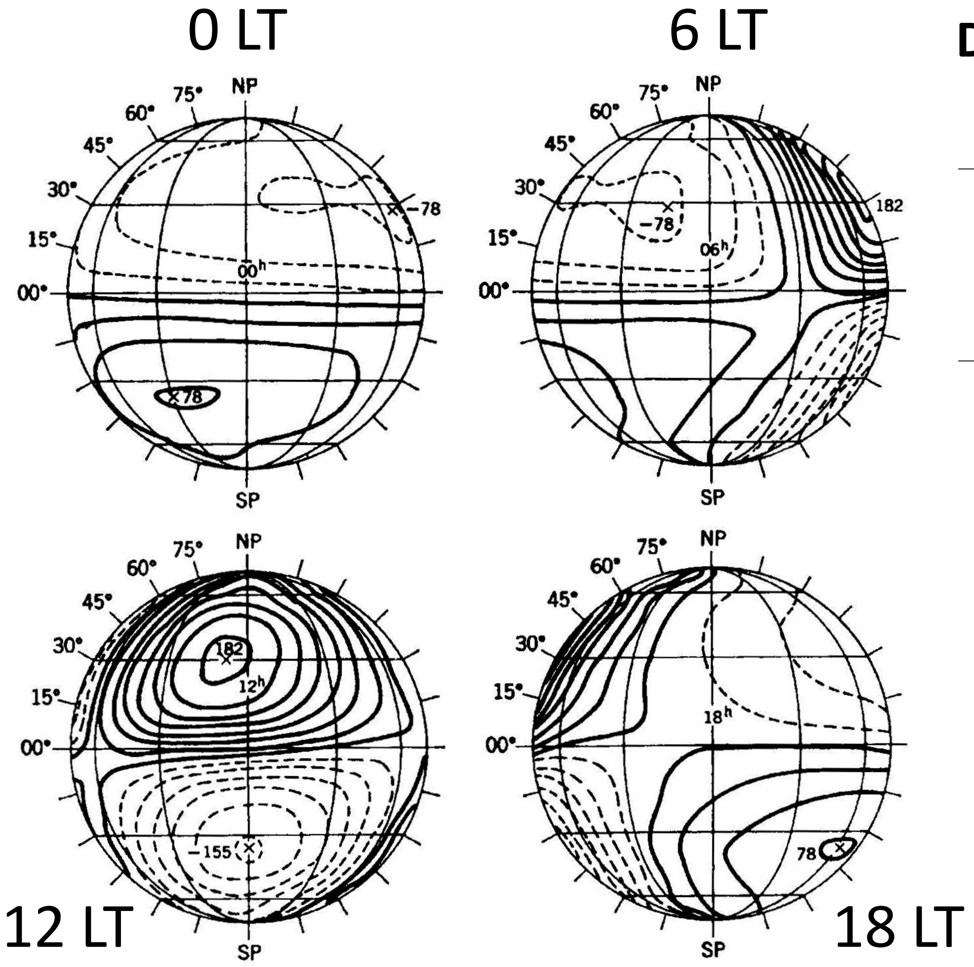

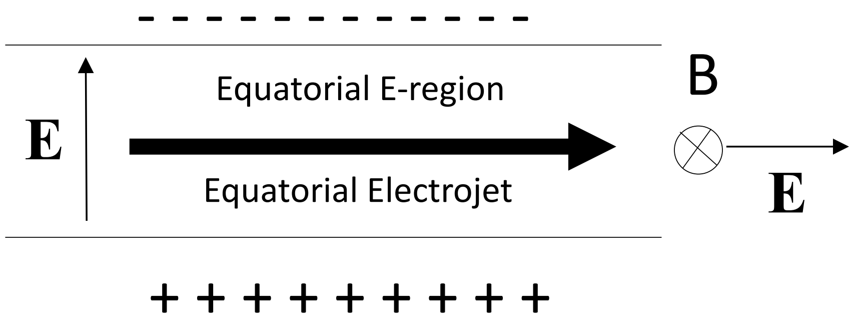

Fig. 7.21. Average mean S_q (solar quiet) current systems during IGY (International Geophysical Year) viewed from the magnetic equator at the 00, 06, 12, and 18 local time meridians. The numbers near the crosses indicate vortex current intensity in 10^3 A. The distance between the current lines corresponds to 2.5×10^3 A. (From Matsushita, 1967.)

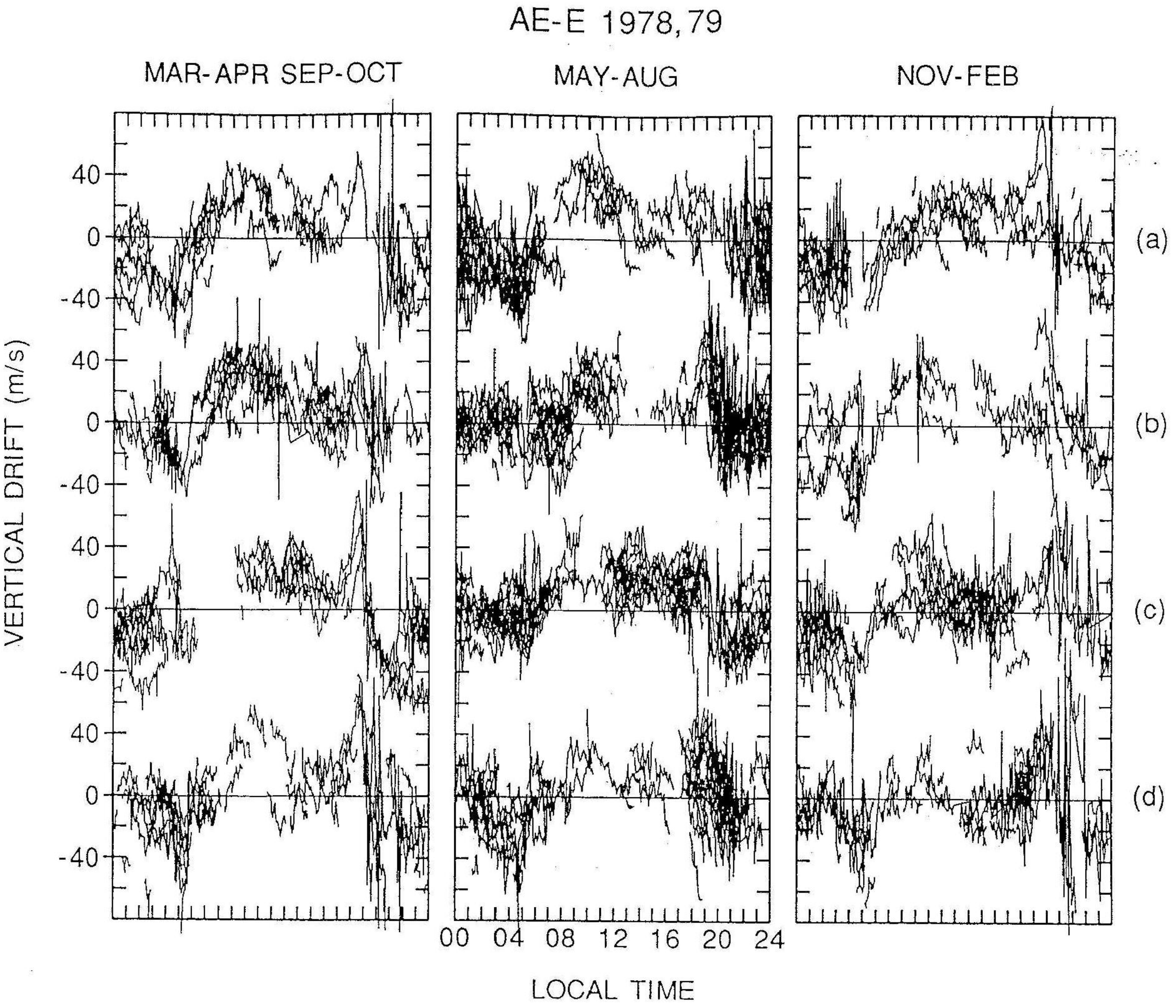
AE-E 1978,79
MAR-APR SEP-OCT
MAY-AUG
NOV-FEB
VERTICAL DRIFT (m/s)
40
0
-40
(a)
(b)
(c)
(d)
00 04 08 12 16 20 24
LOCAL TIME

Fejer et al.

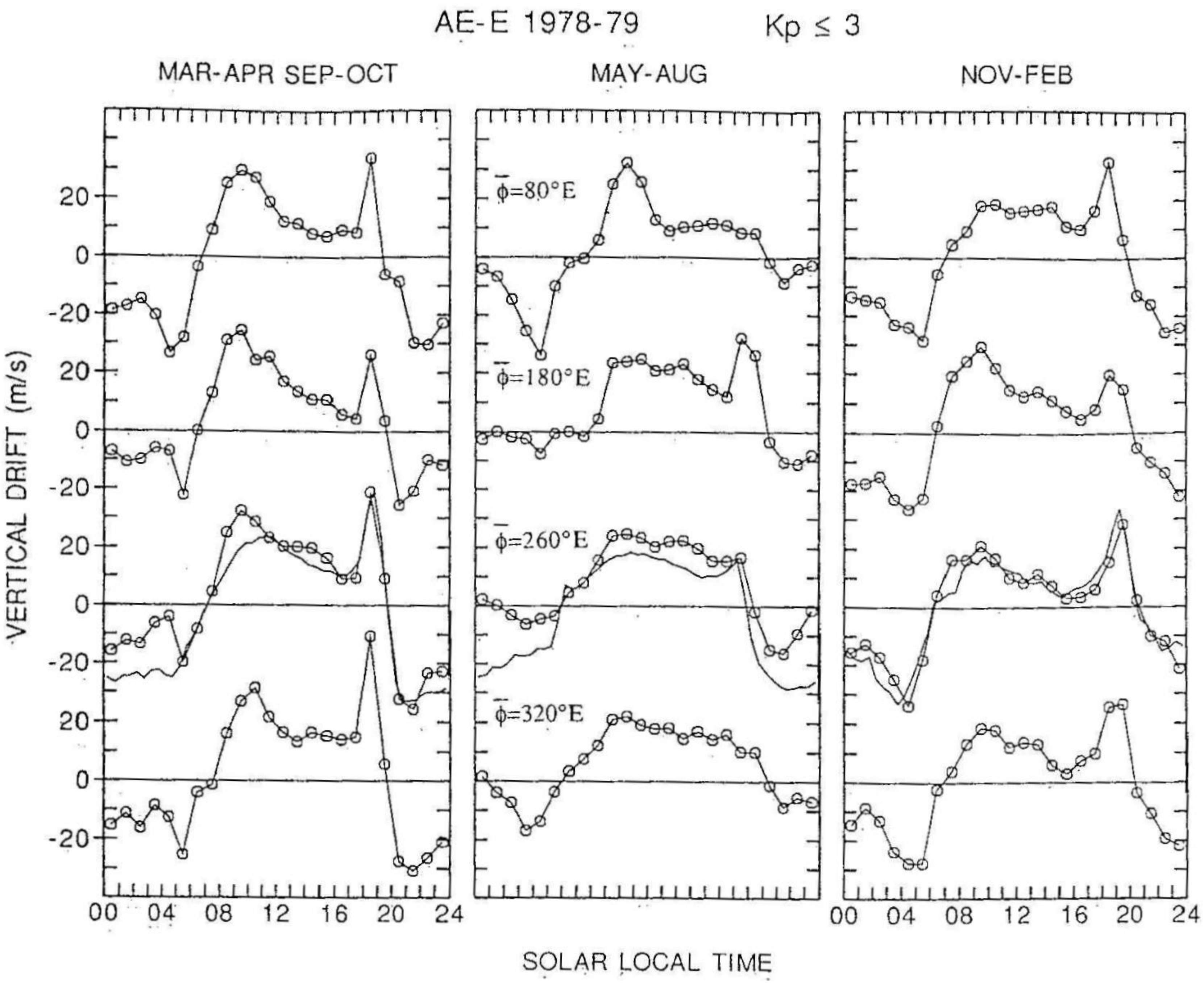

AE-E 1978-79
Kp ≤ 3
MAR-APR SEP-OCT
MAY-AUG
NOV-FEB
VERTICAL DRIFT (m/s)
φ=80°E
φ=180°E
φ=260°E
φ=320°E
SOLAR LOCAL TIME

Fejer et al.

F-Region Dynamo

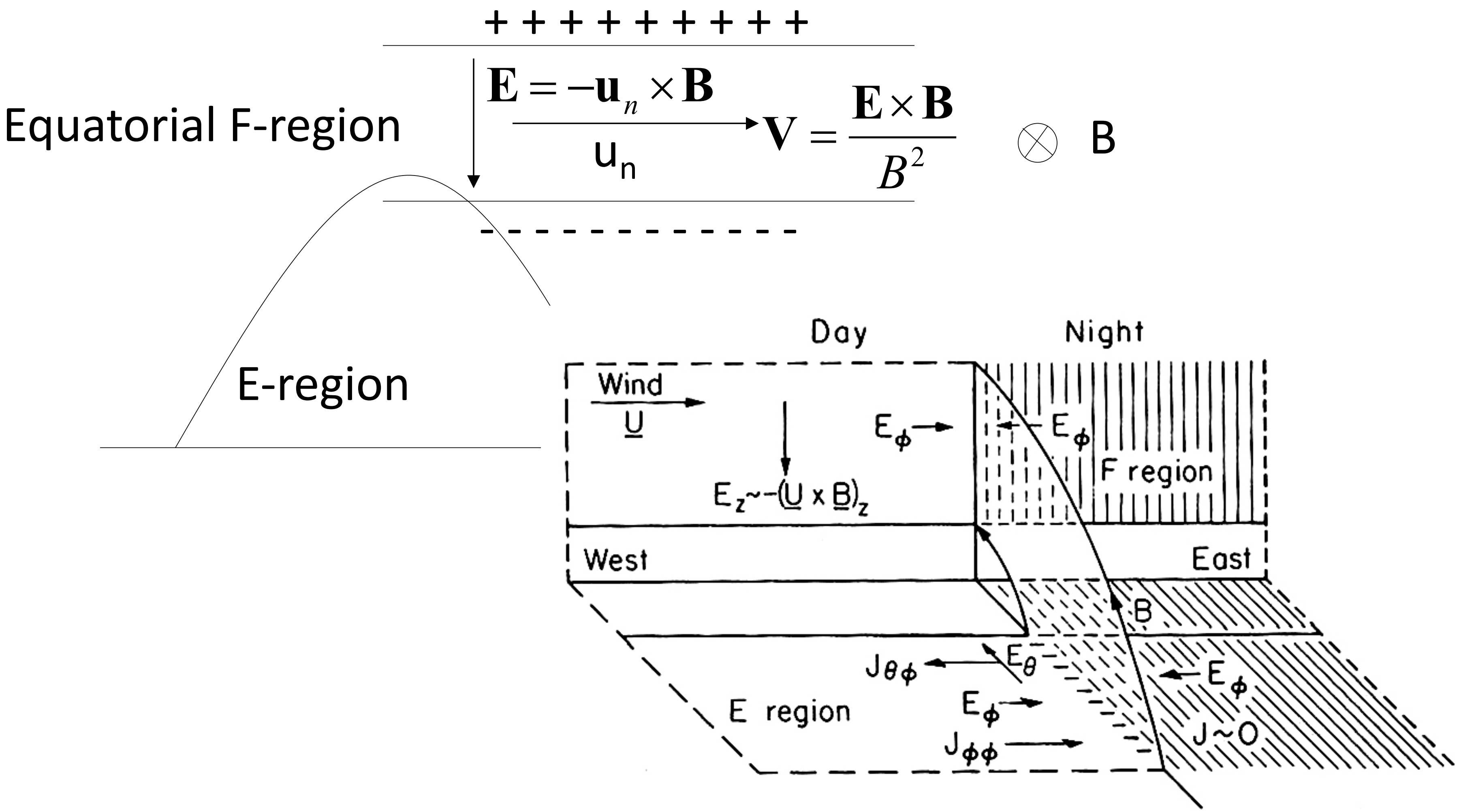

Equatorial Anomaly

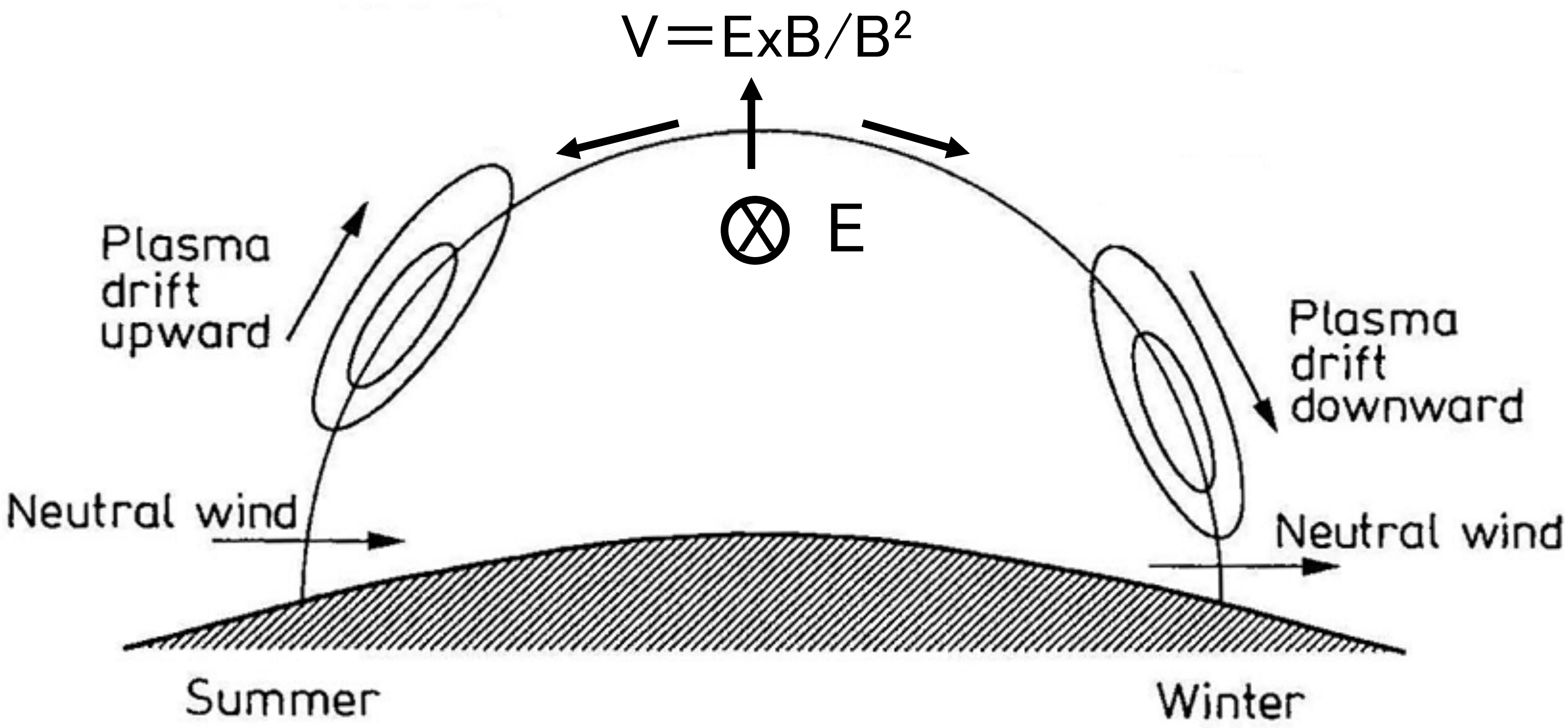

The Earth's Nighttime Equatorial Anomaly Crests as Seen in 1356 Å Light - Photographed from the Moon

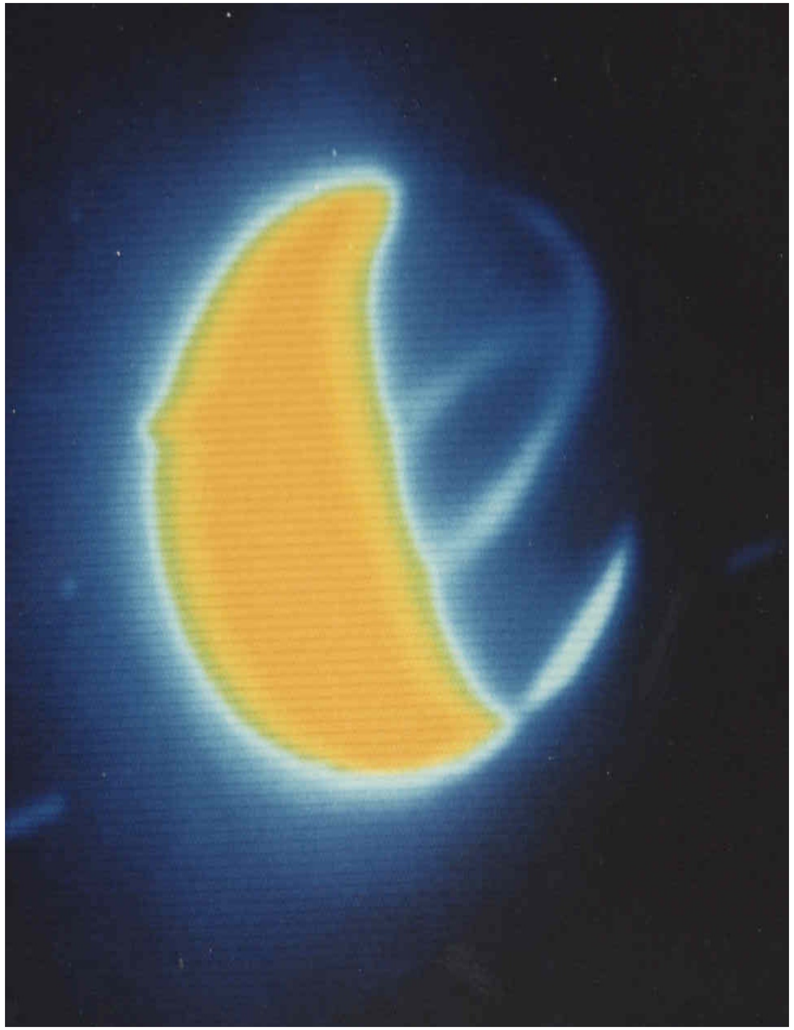

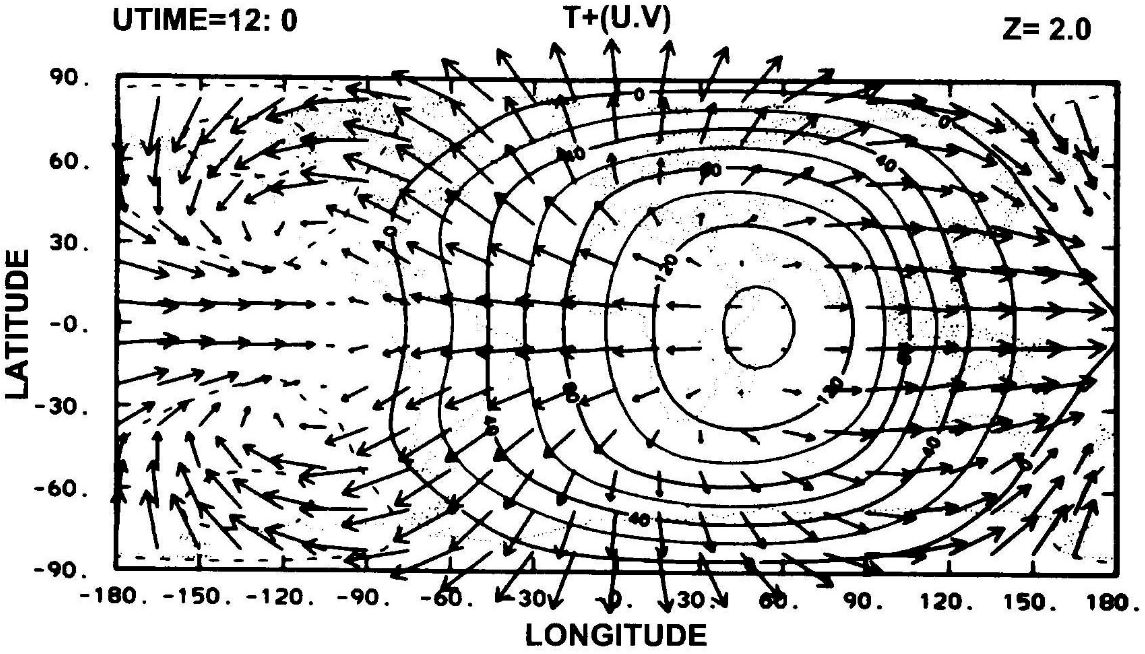

(a)

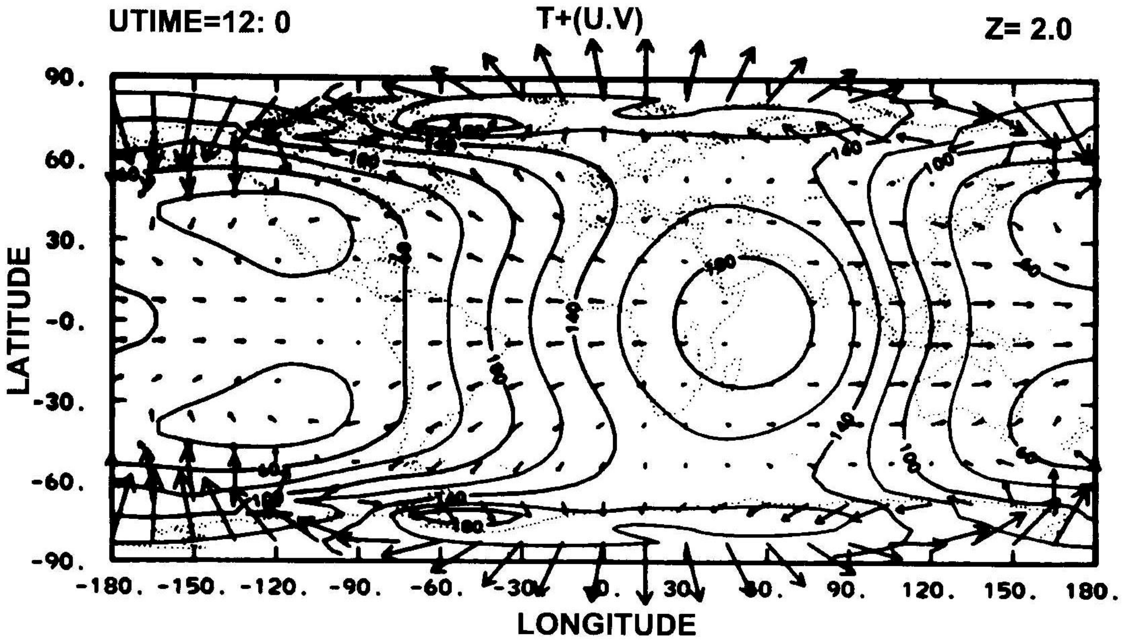

(b)

~300km altitude
(a) 100m/s maximum
(b) 336m/s maximum
60kV cross-tail
potential

Geomagnetic Activity

Quiet

Average

Storm

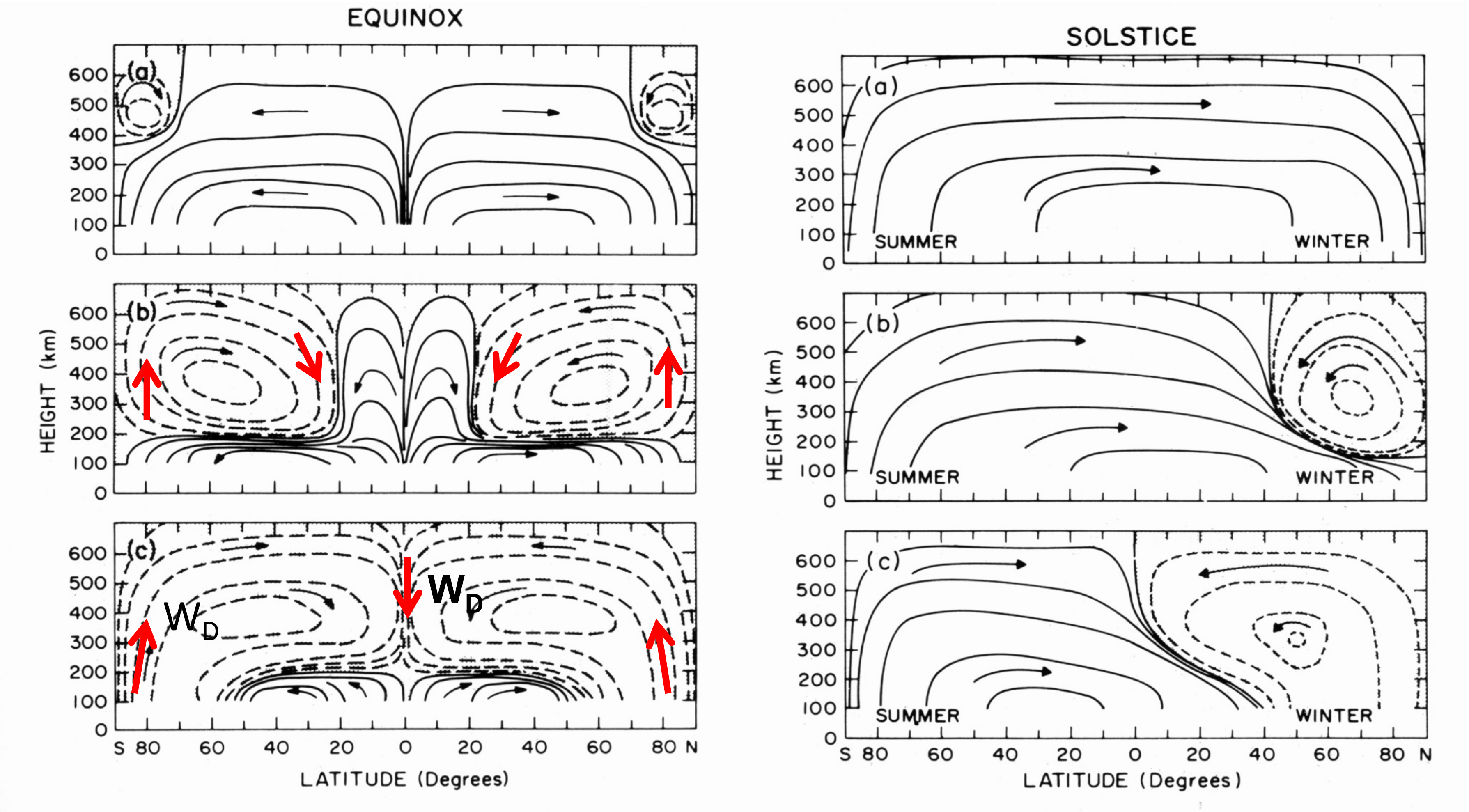

Negative Ionospheric Storm

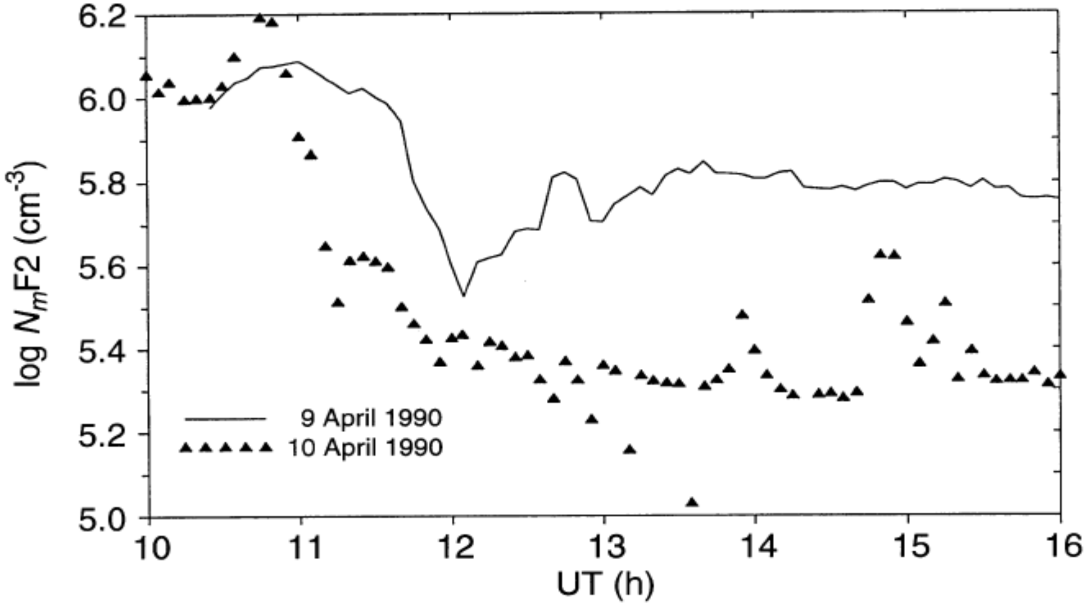

EISCAT

A. Mikhailov, K. Schlegel
Ann. Geophysicae, 1998

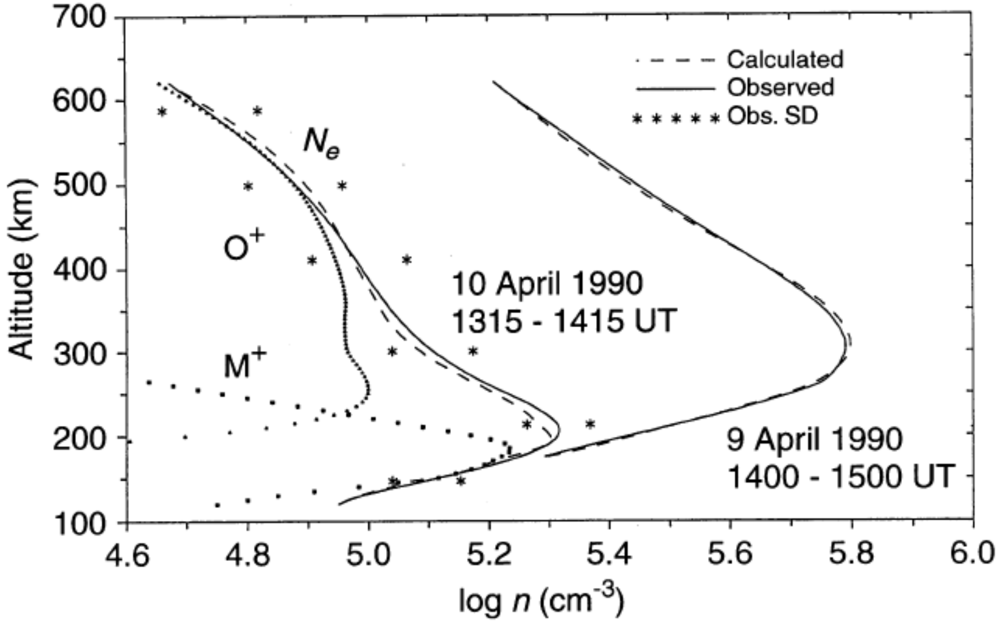

Electron density decrease during the decrease of O/N_2

Photochemistry in the Upper Atmosphere

Photoionization by EUV

$$O + h\nu \rightarrow O^+ + e$$

$$O_2 + h\nu \rightarrow O_2^+ + e$$

$$N_2 + h\nu \rightarrow N_2^+ + e$$

$$He + h\nu \rightarrow He^+ + e$$

Radiative Recombination

$$O^+ + e \rightarrow O + h\nu$$

$$He^+ + e \rightarrow He + h\nu$$

$$H^+ + e \rightarrow H + h\nu$$

Electron-Ion Recombination

$$NO^+ + e \rightarrow N + O$$

$$O_2^+ + e \rightarrow O + O$$

$$N_2^+ + e \rightarrow N + N$$

Ion-Molecule Reactions

$$O^+ + N_2 \rightarrow NO^+ + N$$

$$O^+ + O_2 \rightarrow O + O_2^+$$

$$O_2^+ + NO \rightarrow O_2 + NO^+$$

$$N_2^+ + O \rightarrow NO^+ + N$$

$$N_2^+ + O_2 \rightarrow N_2 + O_2^+$$

$$H^+ + O \rightarrow H + O^+$$

Positive Ionospheric Storm

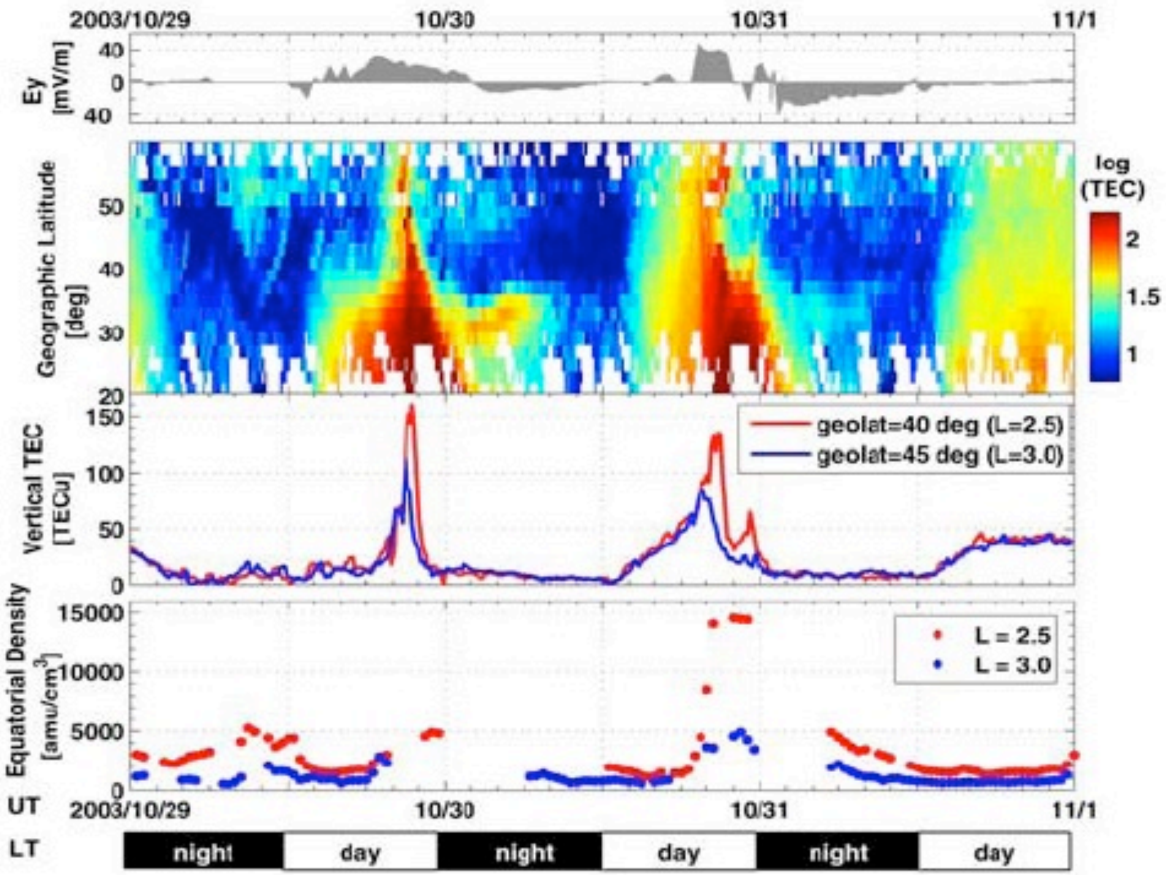

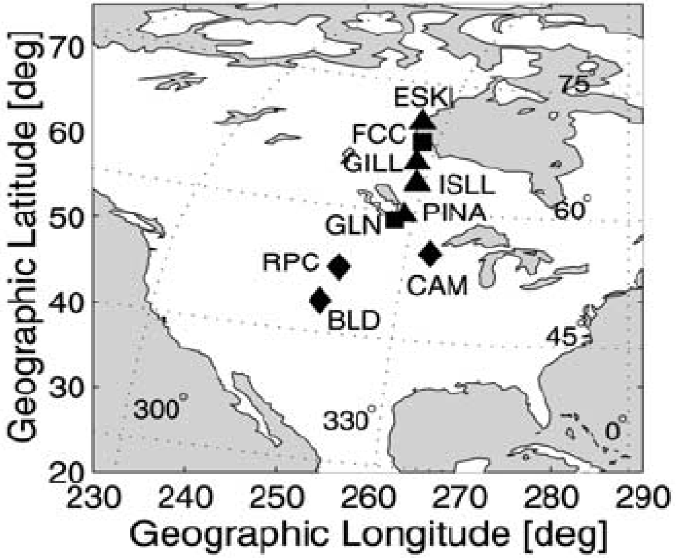

Figure 3. (From top to bottom) The IMF E_y (eastward), the vertical total electron content (TEC) along the 255° geographic longitude, the same vertical TEC values at L = 2.5 and 3.0, and the equatorial plasma density at approximately 255° geographic longitude and at the same L-values inferred by field line resonance measurements.

P. J. Chi et al, 2005

Large Scale Travelling Ionospheric Disturbances (LSTIDs)

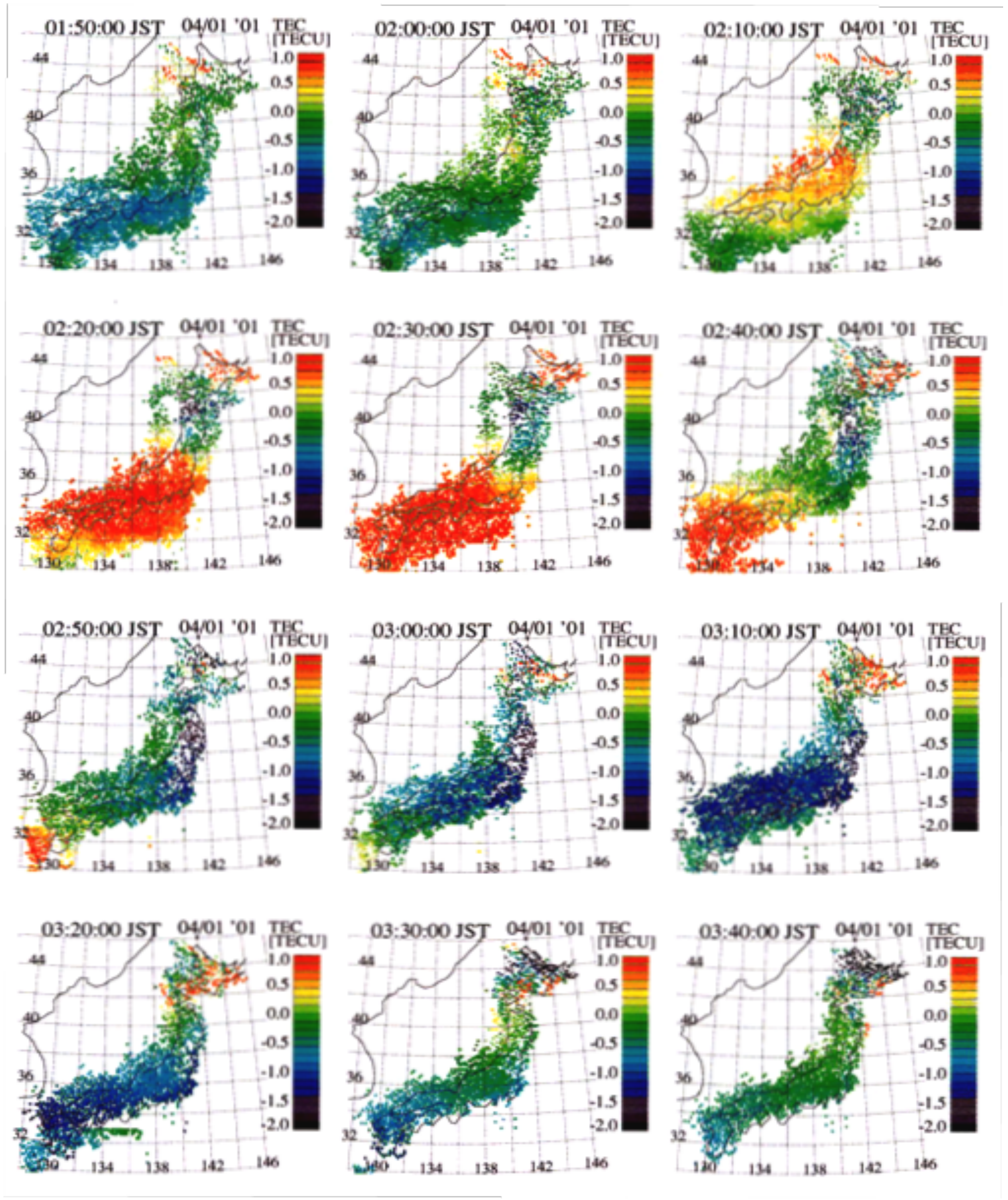

～400m/s

Global Response to Geomagnetic Disturbances

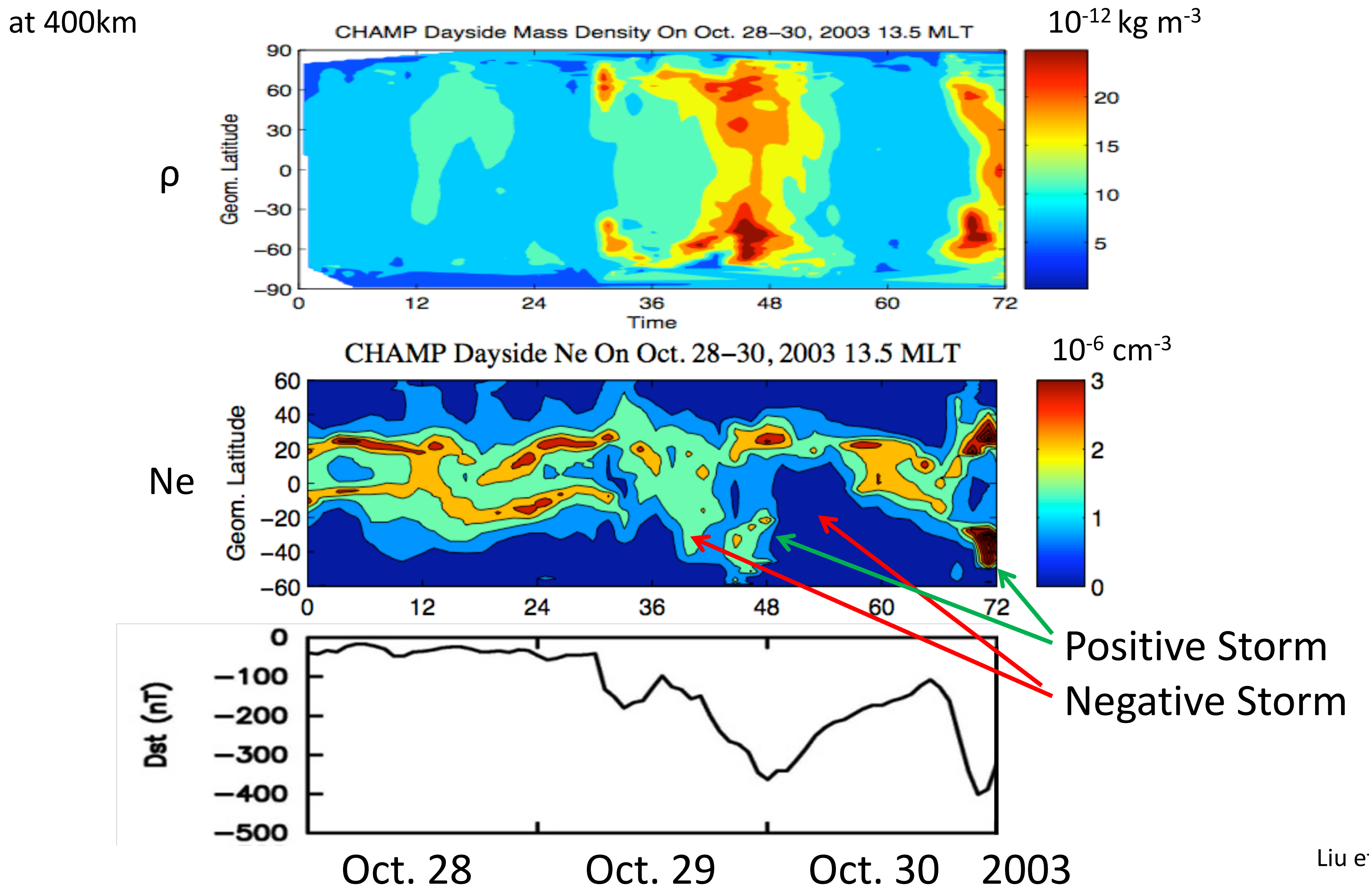

Liu et al.

Ionosphere Thermosphere

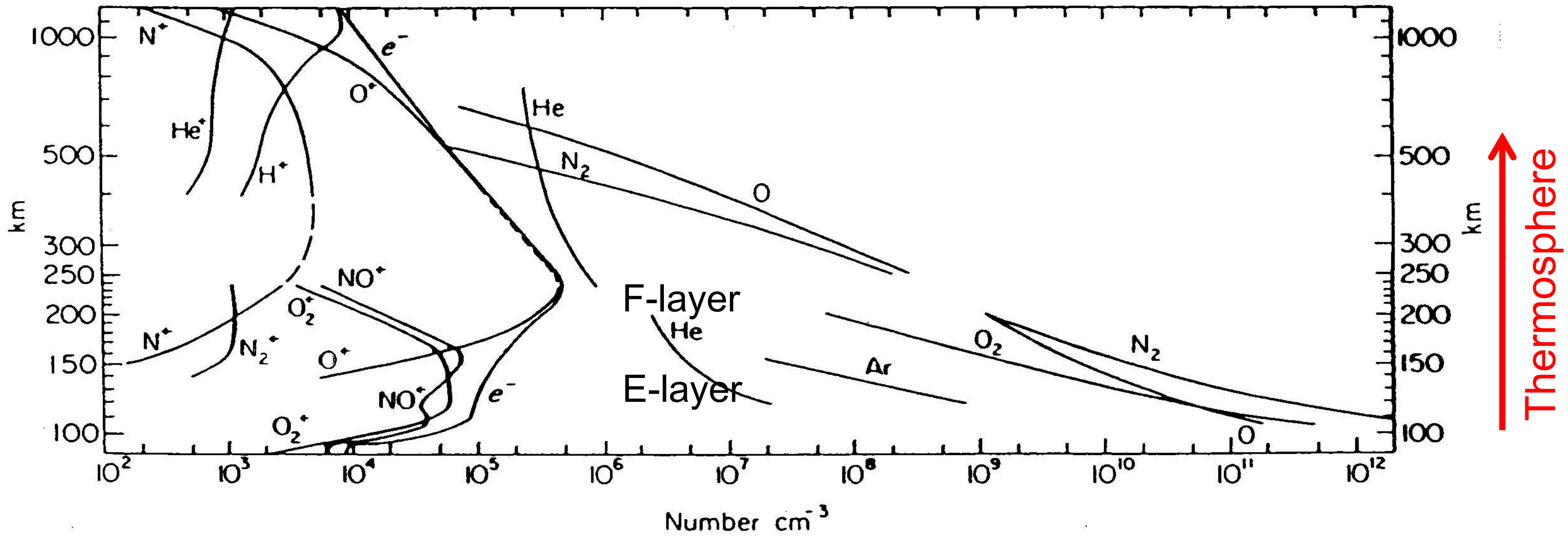

Fig. 1.2. International Quiet Solar Year (IQSY) daytime atmospheric composition, based on mass spectrometer measurements above White Sands, New Mexico (32°N, 106°W). The helium distribution is from a nighttime measurement. Distributions above 250 km are from the Elektron II satellite results of Istomin (1966) and Explorer XVII results of Reber and Nicolet (1965). [C. Y. Johnson, U.S. Naval Research Laboratory, Washington, D.C. Reprinted from Johnson (1969) by permission of the MIT Press, Cambridge, Massachusetts. Copyright 1969 by MIT.]

Although the ionization rate is <10^{-4} in the low latitude thermosphere, the dynamics of the neutral atmosphere is strongly controlled by the plasma.

Neutral Density Anomaly

at 400km

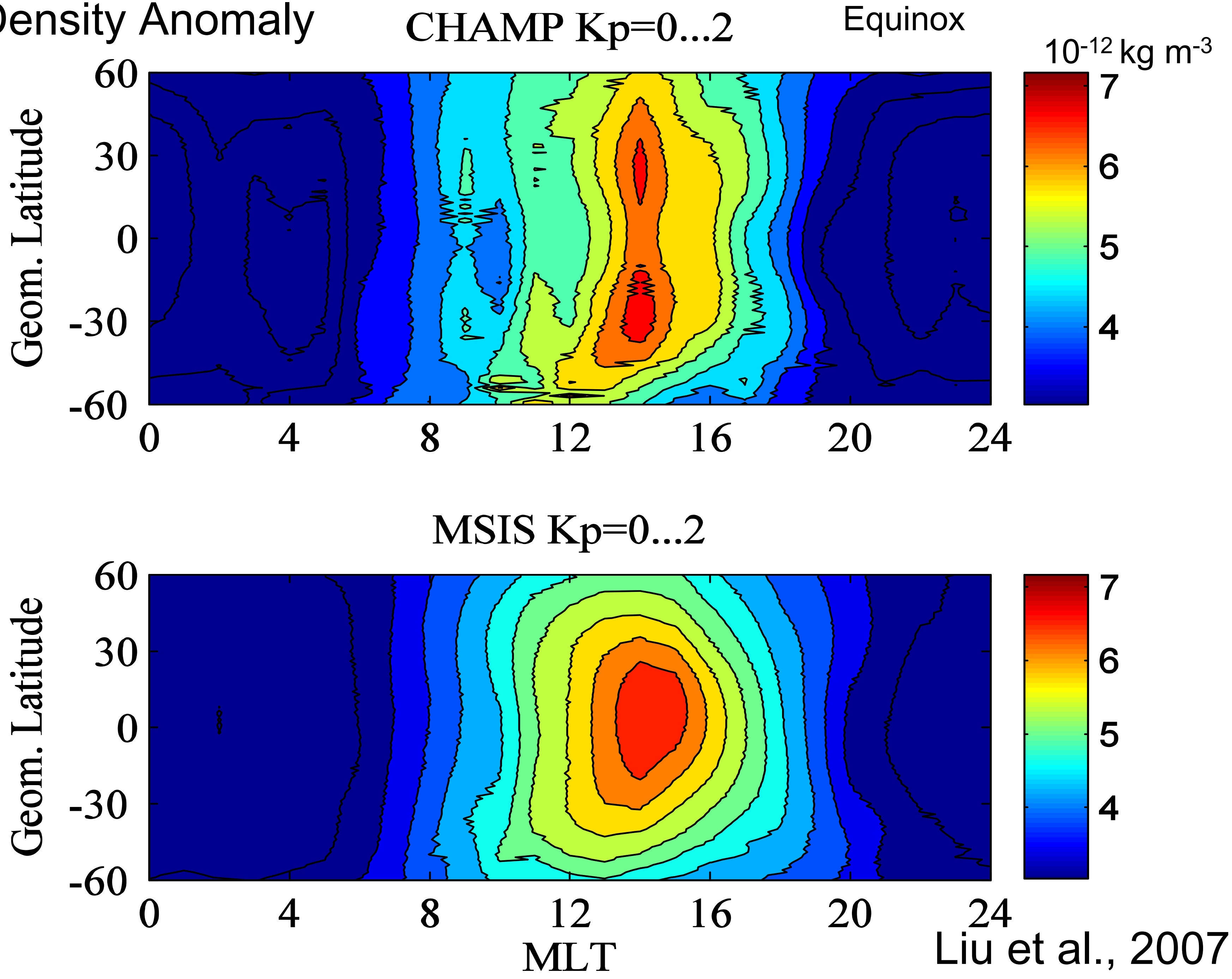

Liu et al., 2007

Neutral Mass Density

Electron Density

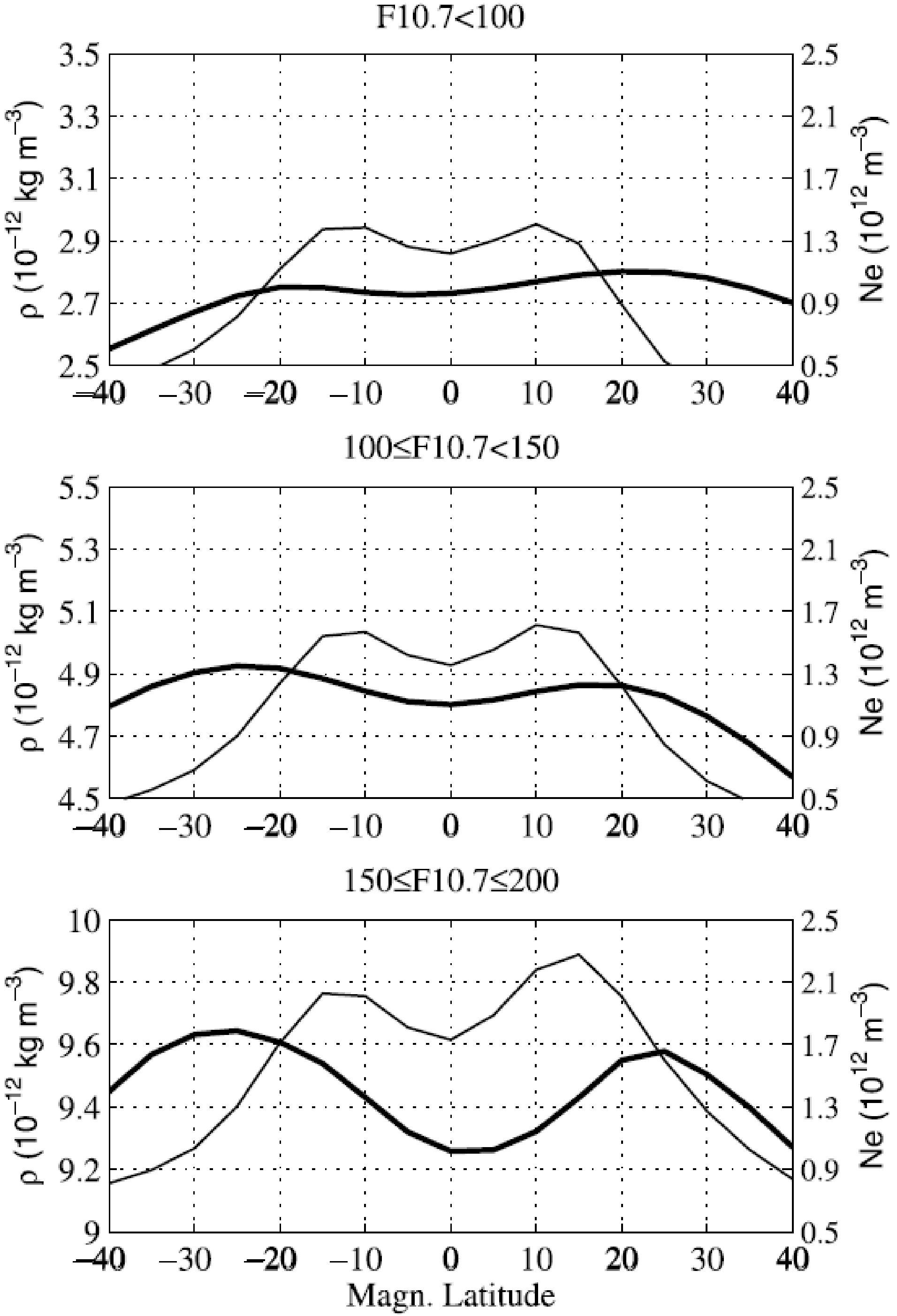

at 400km
11-16 LT
Equinox

Liu et al., 2007

Fast Thermospheric Wind Jet at the Earth's Dip Equator
(Zonal Neutral Wind)

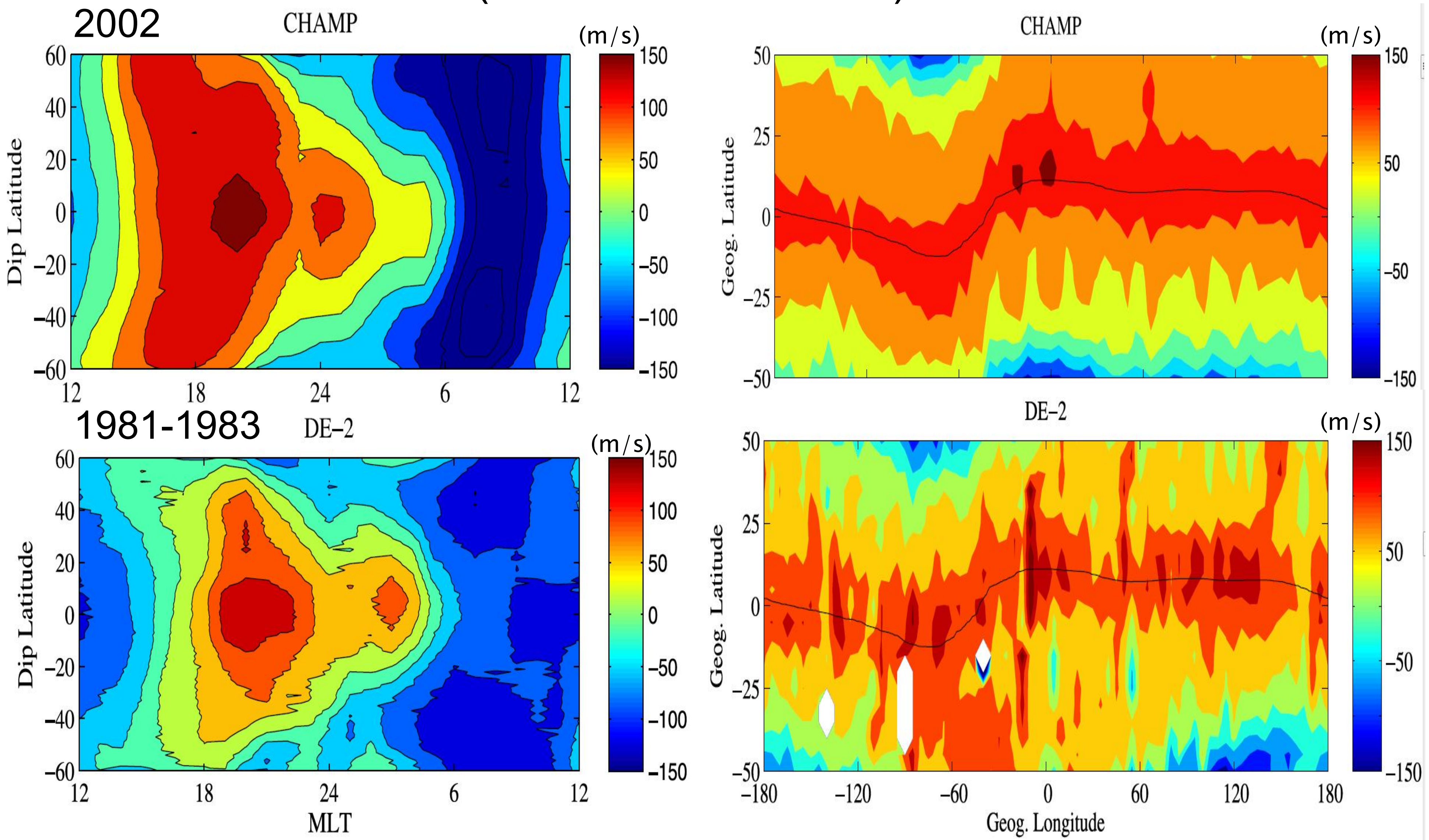

Accelerometer on CHAMP, Wind and Temperature Spectrometer on DE2

Liu et al., 2009

Atmospheric Super-rotation at 400 km altitude

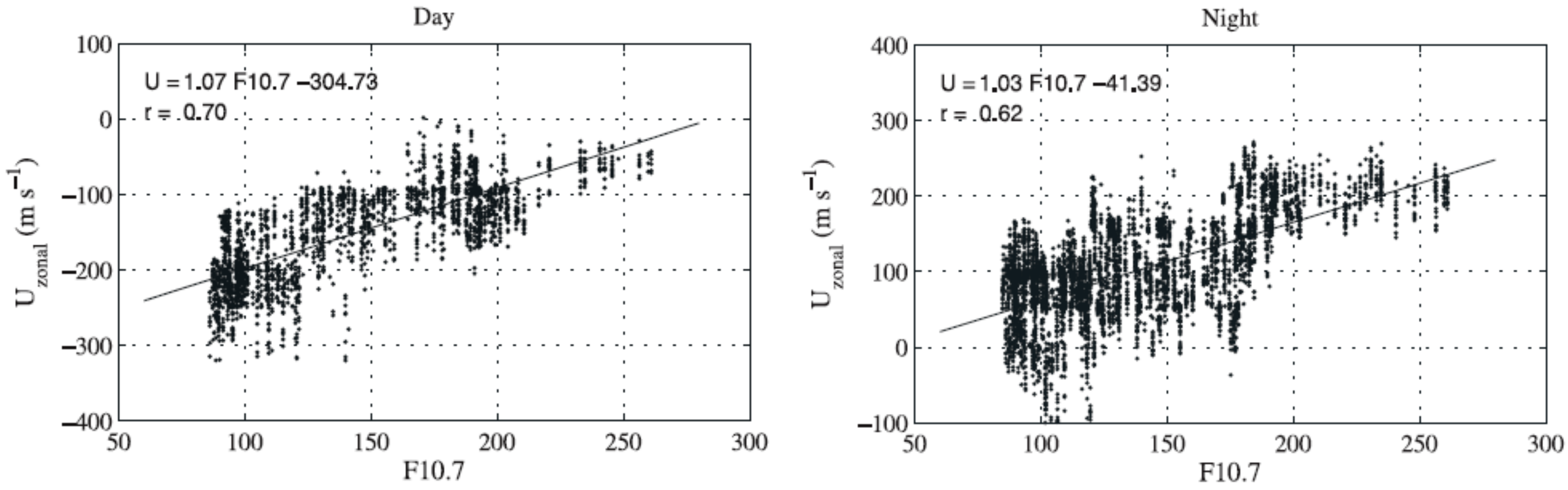

	Summer	Equinox	Winter	Average
F10.7<140	11	22	34	22
F10.7>140	40	72	76	63

(m/s)

fastest in winter at high solar flux level

Liu et al., 2006

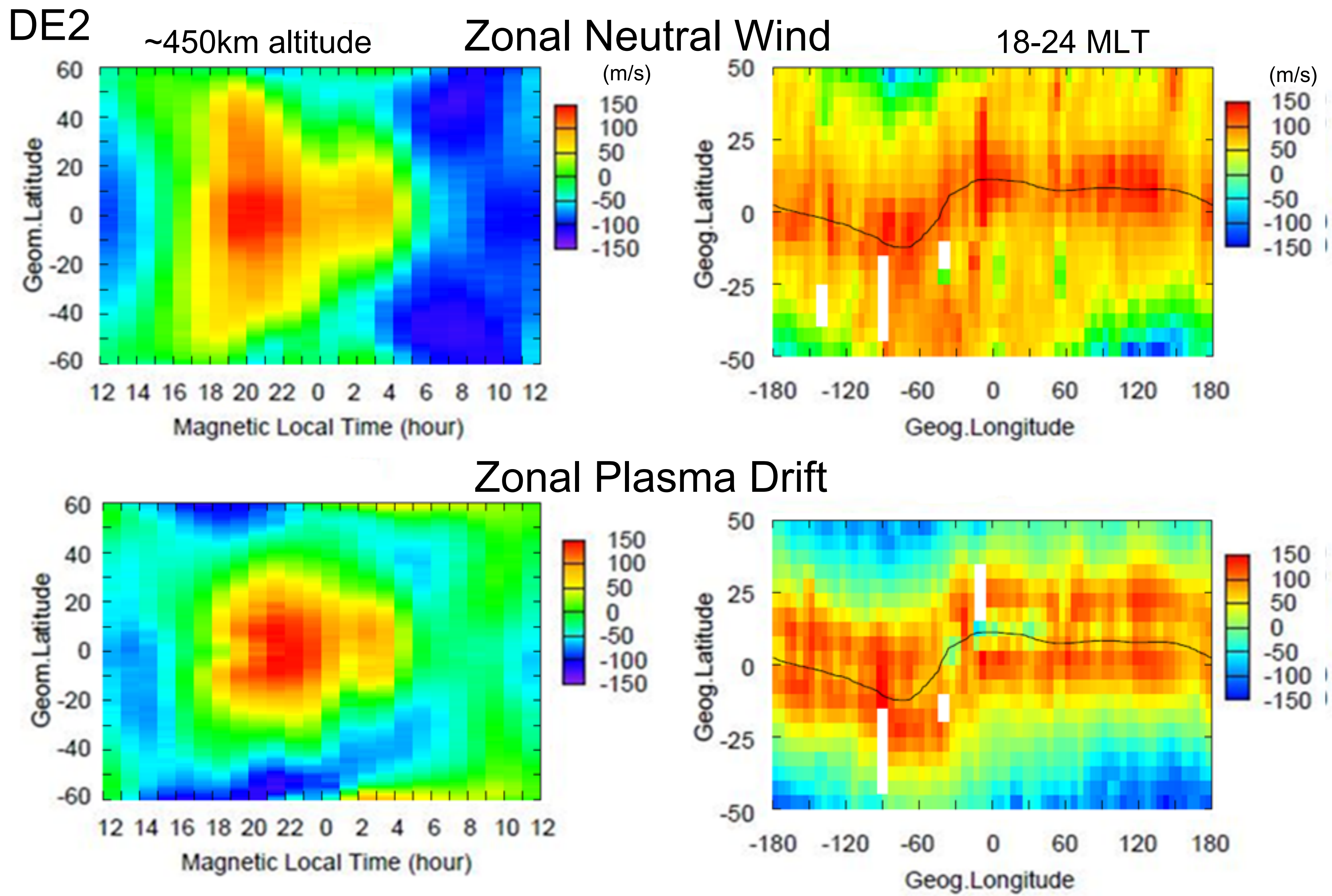

Watanabe and Kondo, 2011

Lithium/TMA Release Experiments in the Upper Atmosphere

2007/9/2	19:20LT	WINDs-1 (KSC)	Lithium
2012/1/12	6:00LT	WINDs-2 (KSC)	Lithium
2013/5/7	19:39LT	EVEX (Kwajalein)	Lithium
	19:40:30LT		TMA
2013/7/4	14:30LT	Daytime Dynamo (Wallops)	Lithium
2013/7/20	23:00LT	E-F Coupling (KSC)	TMA
	00:00		Lithium
2014/11/24	8:00LT	C-REX (Norway)	Ba, Sr


2012/01/12 Uchinoura

E-F Region Coupling: 2013/7/20 at Uchinoura TMA

Winds in the mesosphere and the lower thermosphere

Chemical release
(TMA:Trimethylaluminium)

HWM model

WINDs
(Lithium/TMA)

Zonal wind

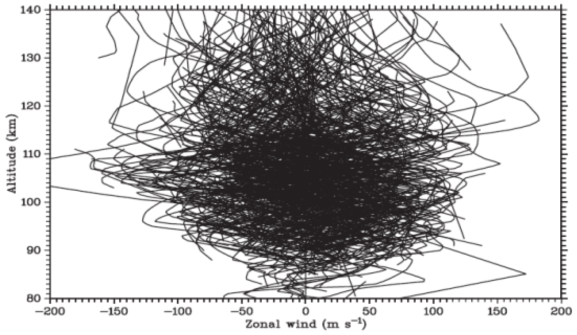

Figure 3. Superposition of the zonal wind components for all the midlatitude and low-latitude chemical release wind profile data.

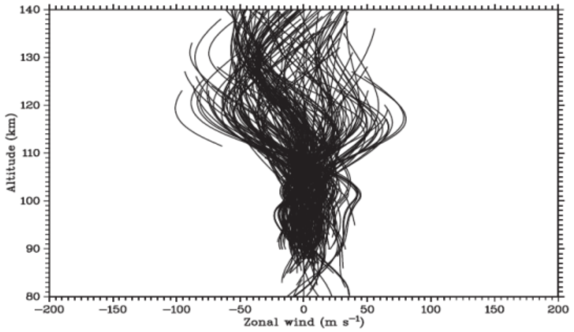

Figure 15. Zonal wind components corresponding to the chemical release wind profiles calculated w HWM.

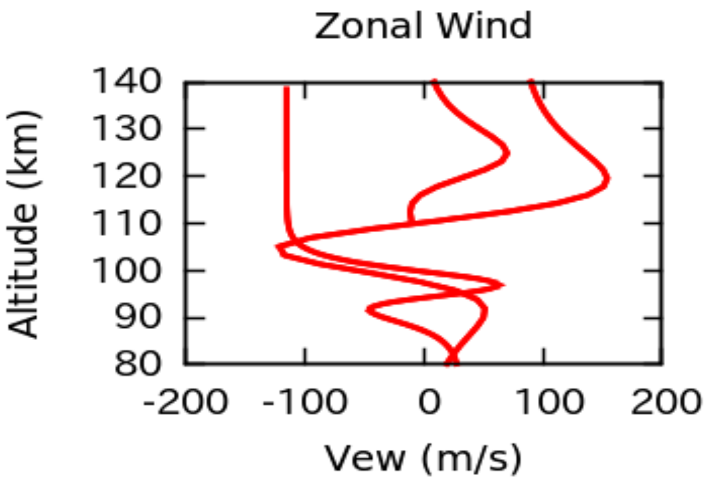

Meridional wind

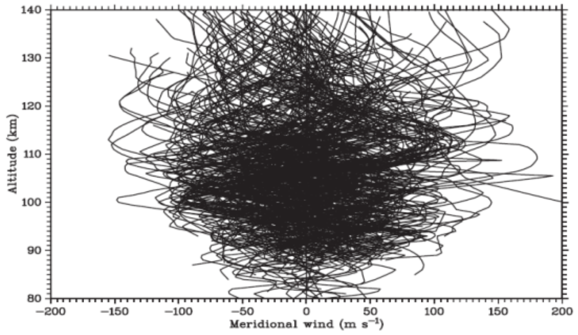

Figure 4. Superposition of the meridional wind components for all the midlatitude and low-latitude chemical release wind profile data.

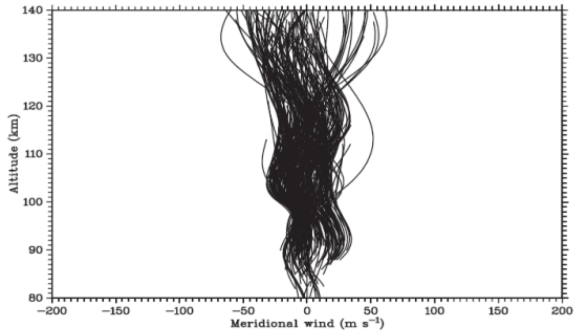

Figure 16. Meridional wind components corresponding to the chemical release wind profiles calcul with HWM.

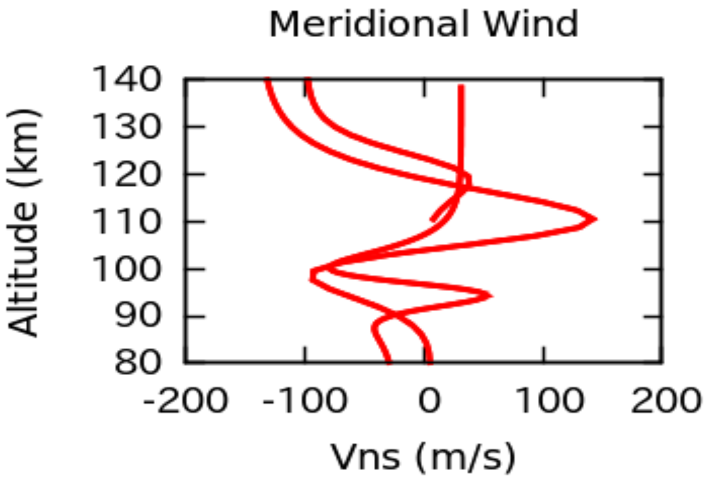

Larsen, 2002

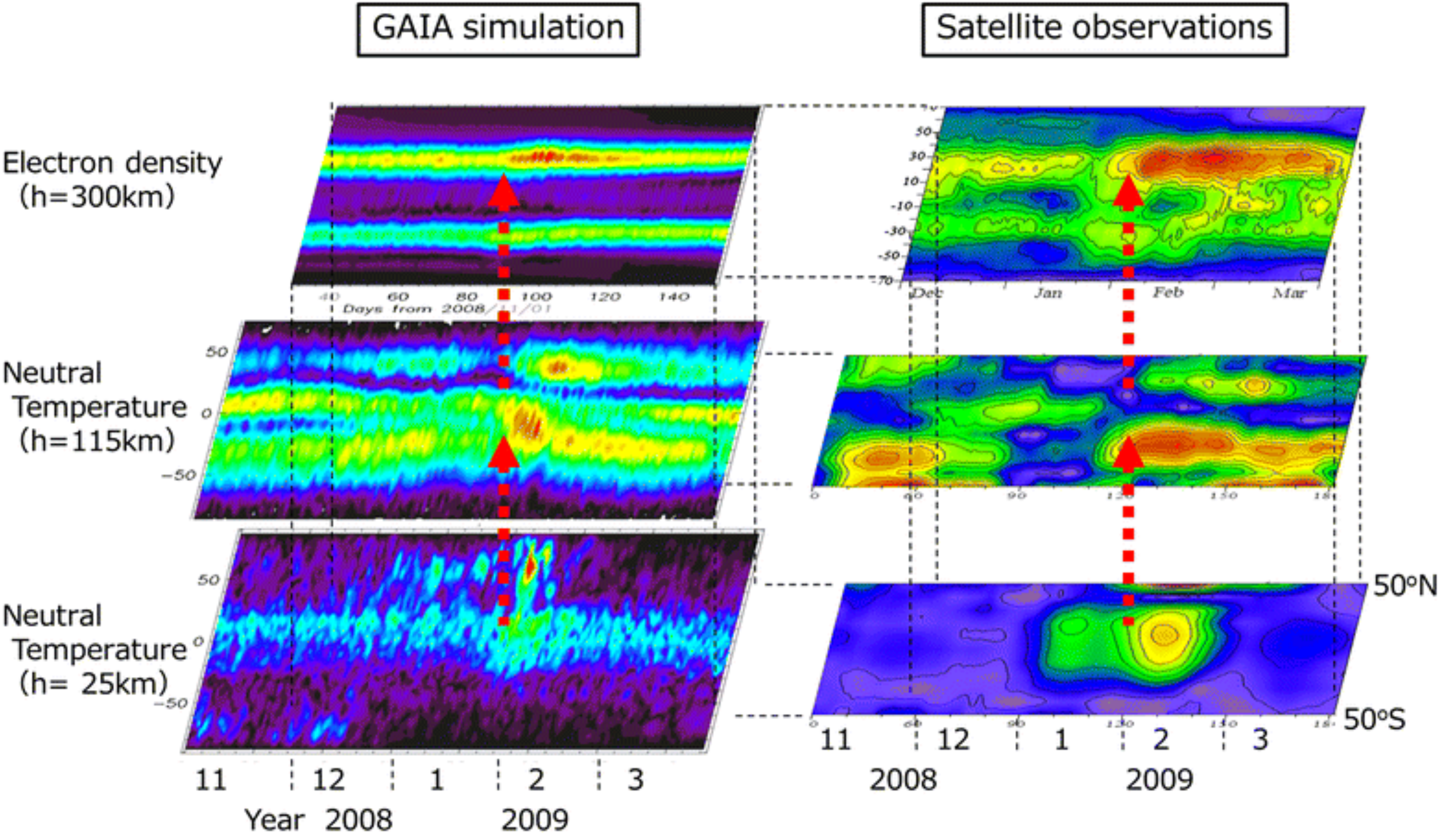

Jin et al., 2012

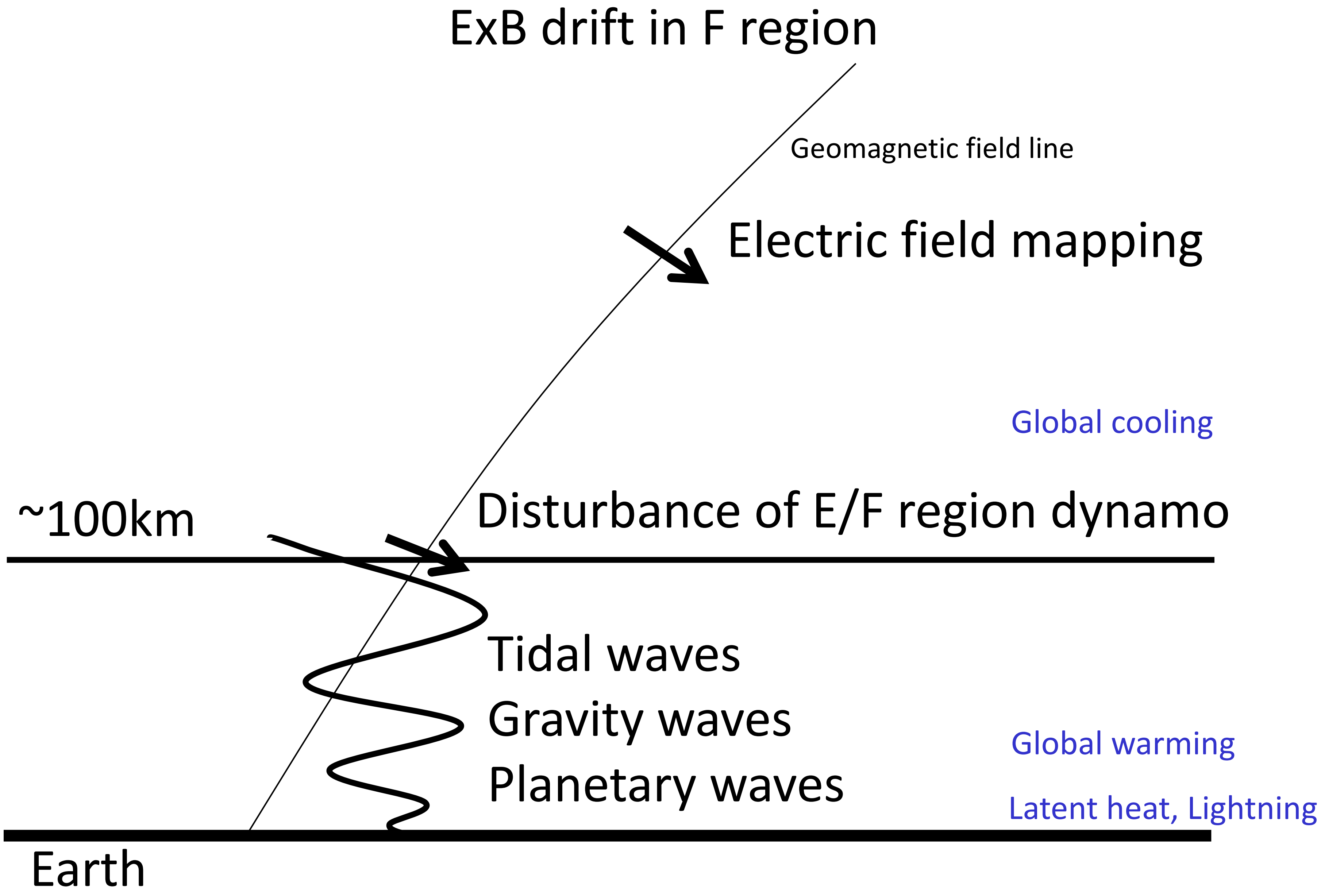
ExB drift in F region
Geomagnetic field line
Electric field mapping
Global cooling
~100km
Disturbance of E/F region dynamo
Tidal waves
Gravity waves
Planetary waves
Global warming
Latent heat, Lightning
Earth

Medium-Scale Traveling Ionospheric Disturbance (MSTID)

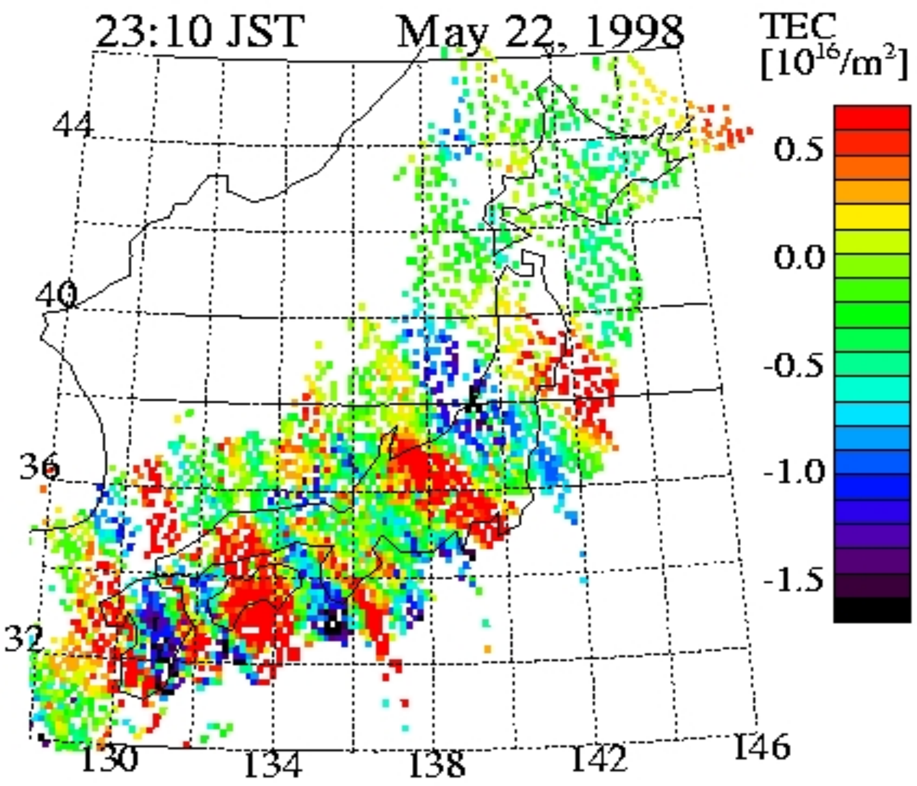

MSTID over Japan

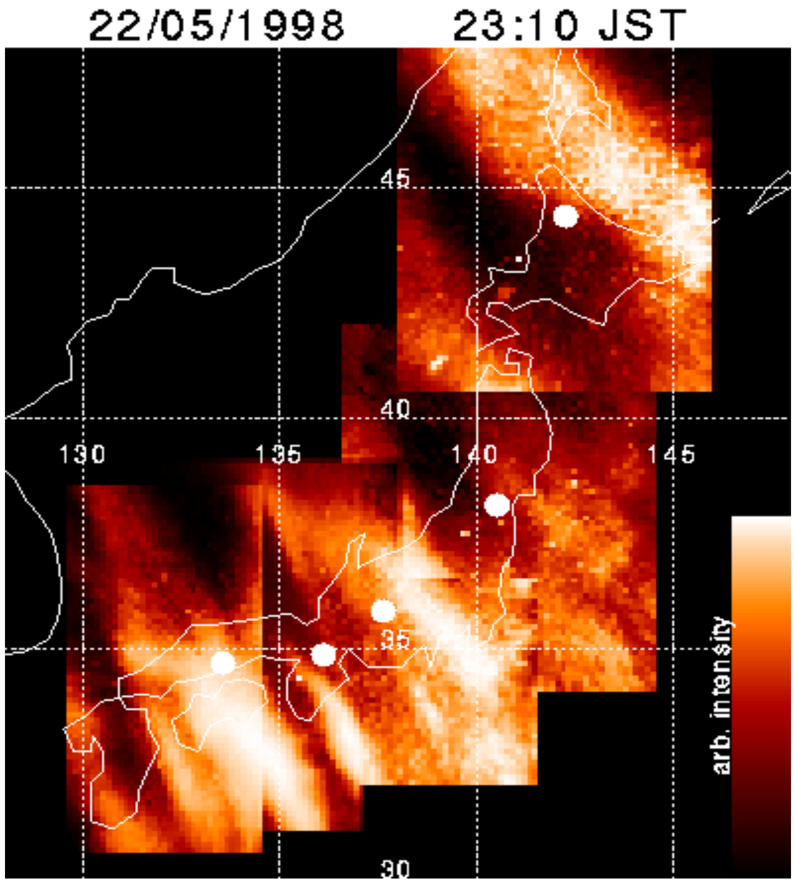

Red Airglow (630nm) over Japan

Saito et al., 2001

MSTID August 9, 2002

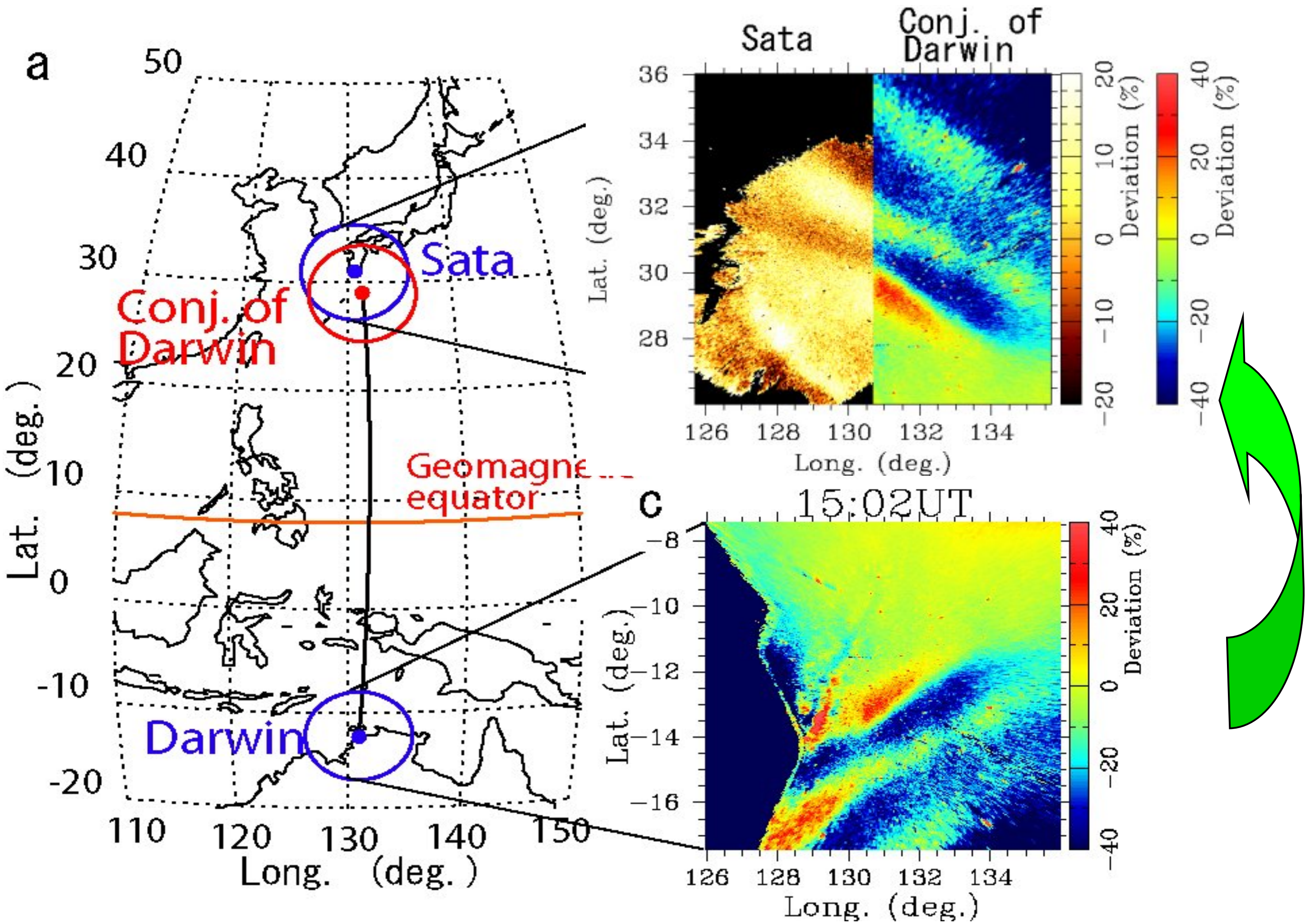

Airglow (630nm)

Otsuka et al., 2005

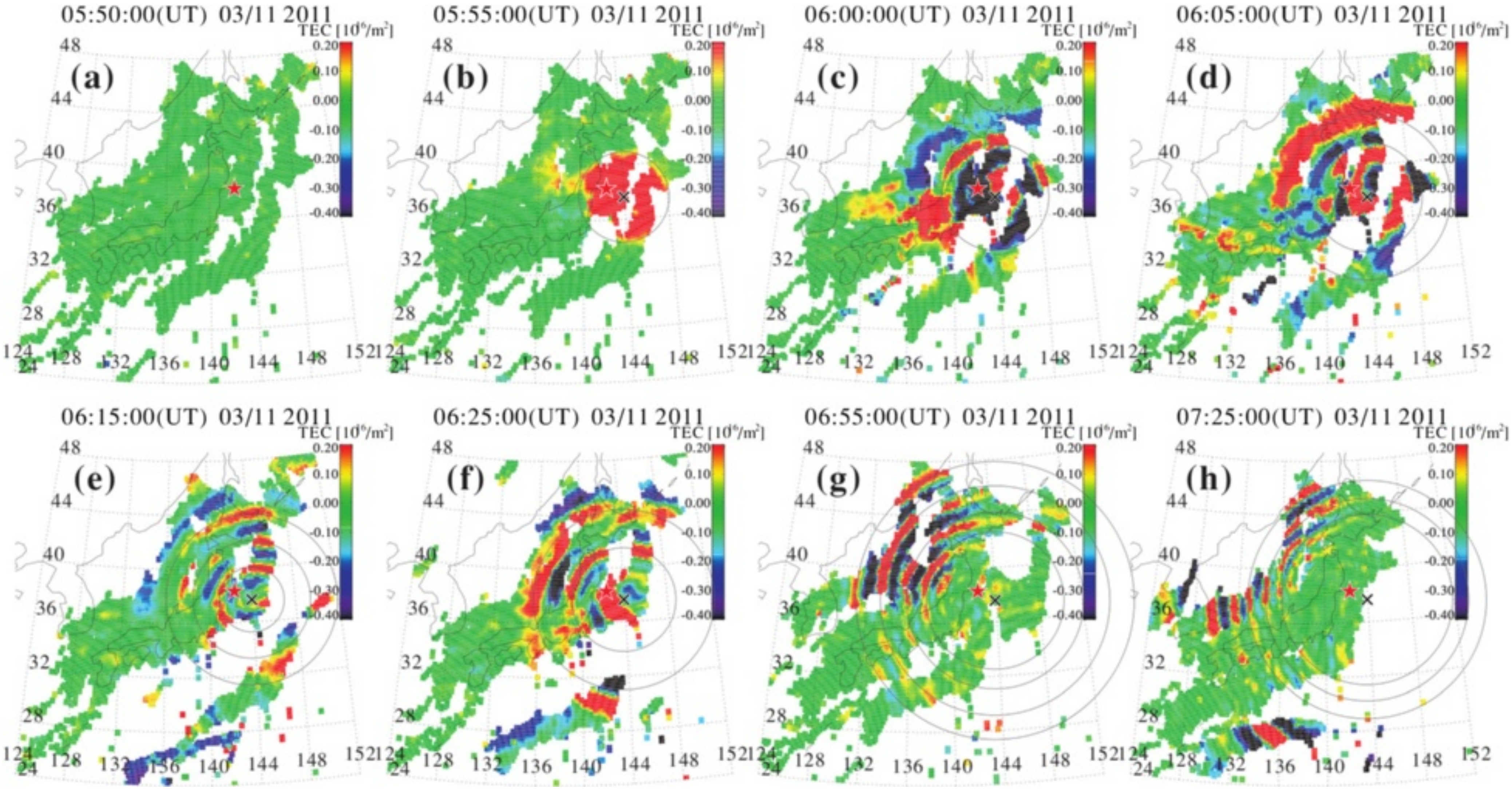

Time series of TEC during the Tohoku Earthquake on March 11, 2011. The star and cross marks represent the epicenter and the ionospheric epicenter, respectively. Gray circles are about the ionospheric epicenter. Tsugawa et al. (2011).

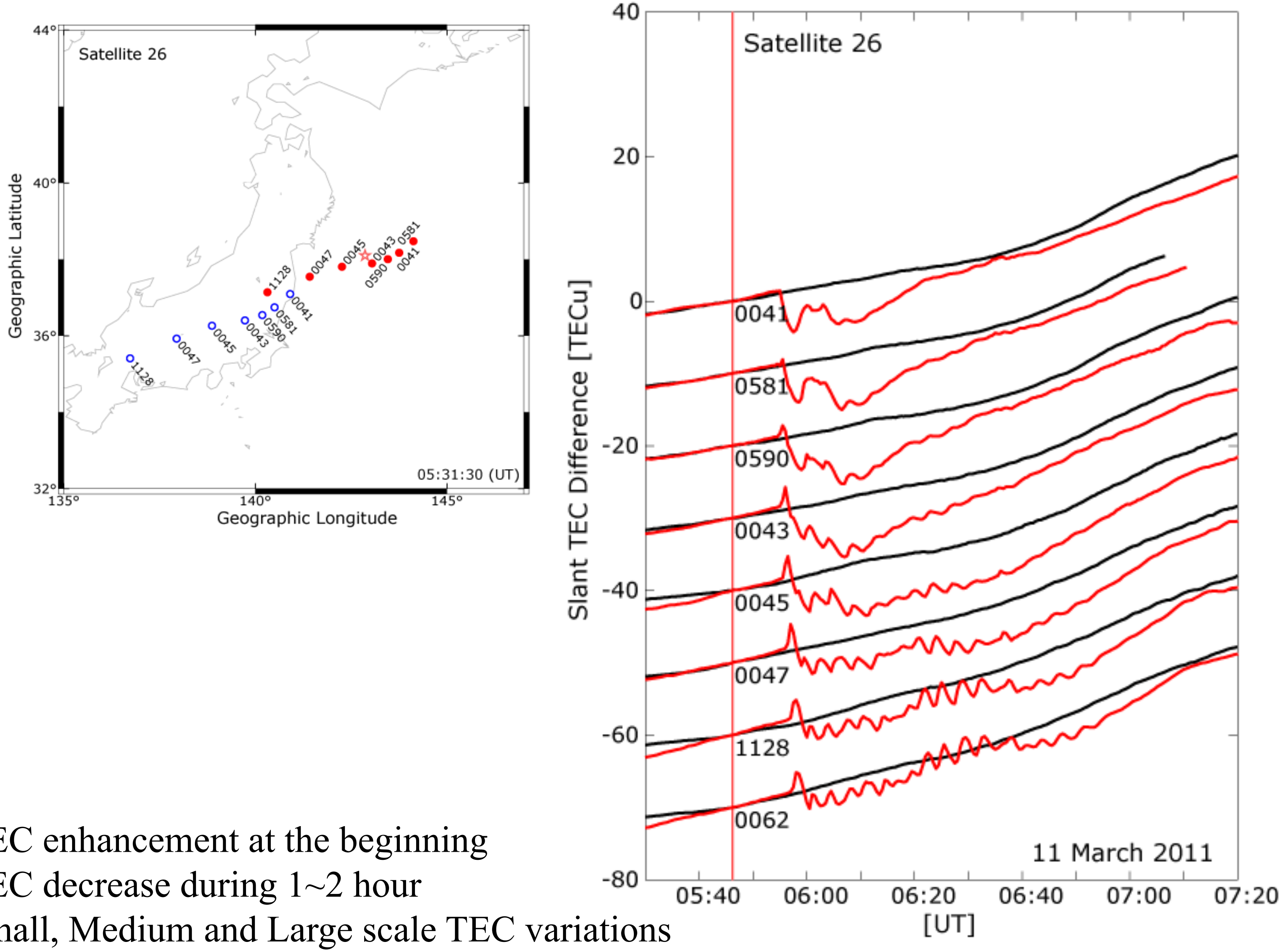

TEC enhancement at the beginning
TEC decrease during 1~2 hour
Small, Medium and Large scale TEC variations

Kakinami et al., 2012

Ionospheric density hole near epicenter

Latitudinal TEC asymmetry

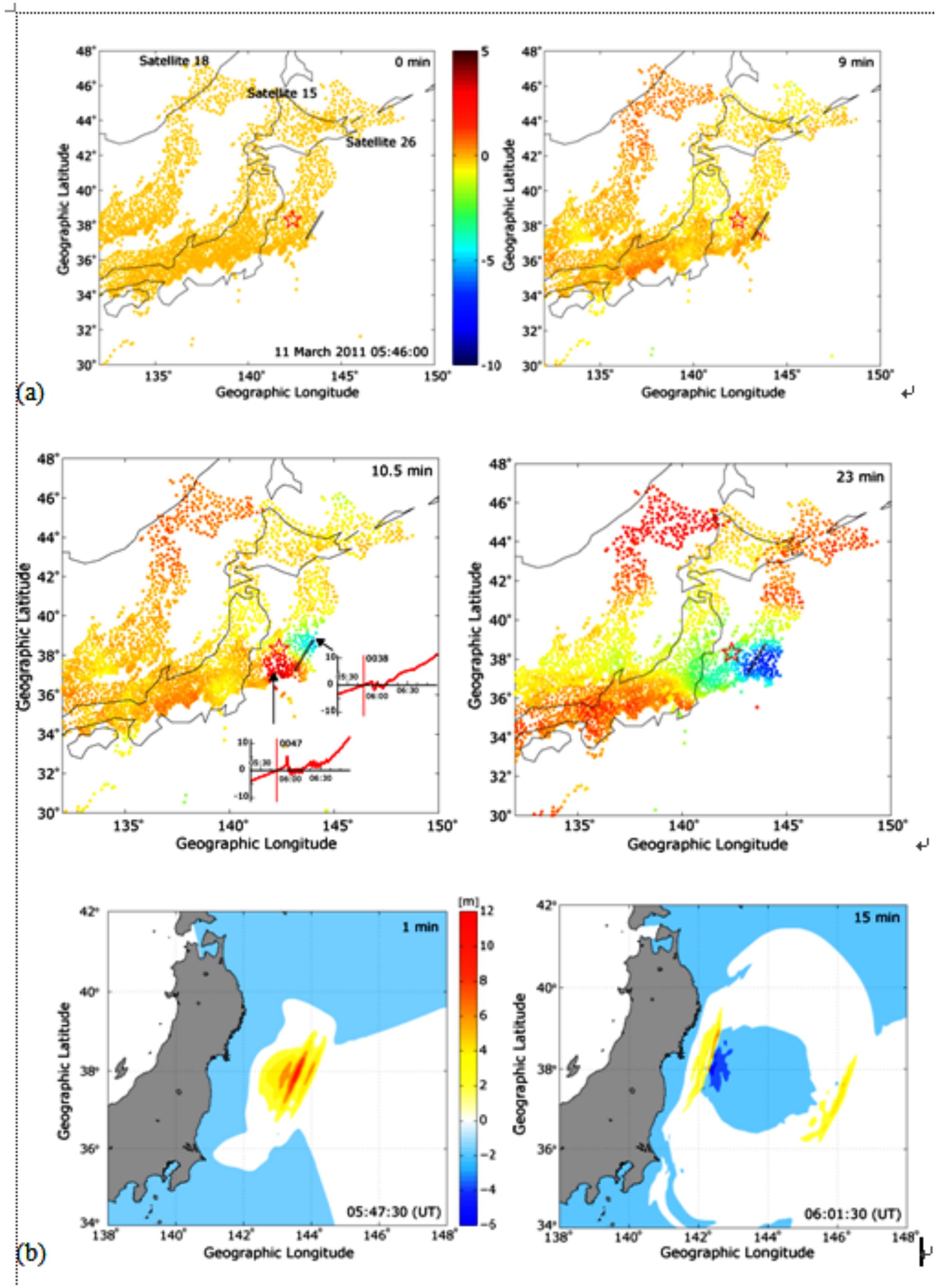

Ionospheric Hole

Tsunami simulation

Kakinami et al., 2012

2.5 Dimensional Model of Neutral Atmosphere/Ionosphere

Neutral Atmosphere

$$\frac{\partial n_n}{\partial t}+u_n\frac{\partial n_n}{\partial x}+v_n\frac{\partial n_n}{\partial y}+w_n\frac{\partial n_n}{\partial z}=-n_n\frac{\partial u_n}{\partial x}-n_n\frac{\partial v_n}{\partial y}-n_n\frac{\partial w_n}{\partial z}$$

$$\frac{\partial u_n}{\partial t}+u_n\frac{\partial u_n}{\partial x}+v_n\frac{\partial u_n}{\partial y}+w_n\frac{\partial u_n}{\partial z}=-\Omega v_n\cos\phi-\frac{1}{\rho_n}\frac{\partial p_n}{\partial x}+\frac{\mu}{\rho_n}\frac{\partial^2 u_n}{\partial x^2}+\frac{\mu}{\rho_n}\frac{\partial^2 u_n}{\partial y^2}+\frac{\mu}{\rho_n}\frac{\partial^2 u_n}{\partial z^2}-\nu_{ni}(u_n-u_i\cos\theta)$$

$$\frac{\partial v_n}{\partial t}+u_n\frac{\partial v_n}{\partial x}+v_n\frac{\partial v_n}{\partial y}+w_n\frac{\partial v_n}{\partial z}=\Omega u_n\cos\phi-\frac{1}{\rho_n}\frac{\partial p_n}{\partial y}+\frac{\mu}{\rho_n}\frac{\partial^2 v_n}{\partial x^2}+\frac{\mu}{\rho_n}\frac{\partial^2 v_n}{\partial y^2}+\frac{\mu}{\rho_n}\frac{\partial^2 v_n}{\partial z^2}-\nu_{ni}v_n$$

$$\frac{\partial w_n}{\partial t}+u_n\frac{\partial w_n}{\partial x}+v_n\frac{\partial w_n}{\partial y}+w_n\frac{\partial w_n}{\partial z}=-\frac{1}{\rho_n}\frac{\partial p_n}{\partial z}+\frac{\mu}{\rho_n}\frac{\partial^2 w_n}{\partial x^2}+\frac{\mu}{\rho_n}\frac{\partial^2 w_n}{\partial y^2}+\frac{\mu}{\rho_n}\frac{\partial^2 w_n}{\partial z^2}-g_0\left(\frac{r_0}{r_0+z}\right)^2-\nu_{ni}(w_n-u_i\sin\theta)$$

$$\frac{\partial p_n}{\partial t}+u_n\frac{\partial p_n}{\partial x}+v_n\frac{\partial p_n}{\partial y}+w_n\frac{\partial p_n}{\partial z}=-\gamma p_n\frac{\partial u_n}{\partial x}-\gamma p_n\frac{\partial v_n}{\partial y}-\gamma p_n\frac{\partial w_n}{\partial z}$$

Ionosphere

$$\frac{\partial n_i}{\partial t}+u_i\frac{\partial n_i}{\partial s}=-n_i\frac{\partial u_i}{\partial s}+Q_i-L_i$$

$$\frac{\partial u_i}{\partial t}+u_i\frac{\partial u_i}{\partial s}=-\frac{1}{\rho_i}\frac{\partial p_i}{\partial s}-g_0\left(\frac{r_0}{r_0+z}\right)^2\sin\theta-\nu_{in}(u_i-u_n\cos\theta-v_n\sin\theta)$$

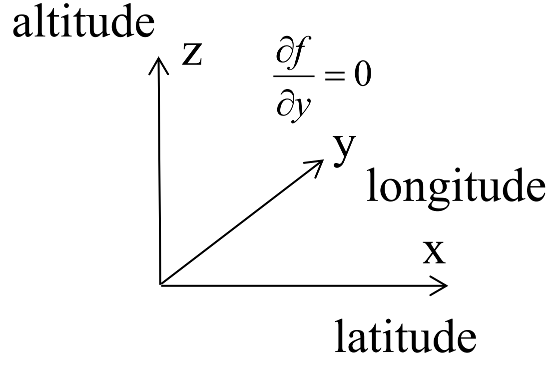

$$\frac{\partial f}{\partial y}=0$$

2.5 Dimensional Model for Neutral Atmosphere - Ionosphere

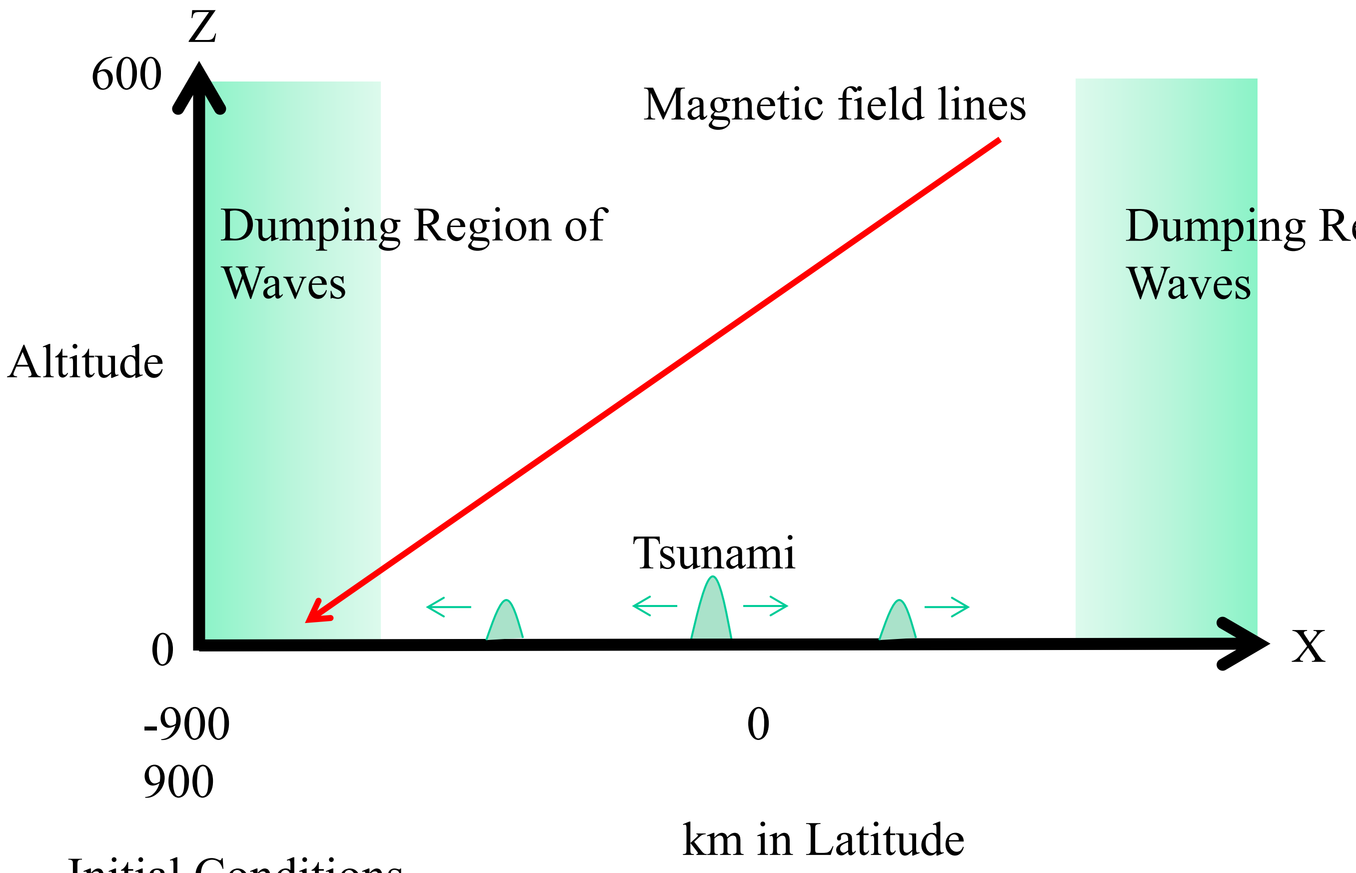

<u>Initial Conditions</u>

Neutral Atmosphere: MSIS model, 2011/3/11, 12LT, Tohoku of Japan

Ionosphere: F layer, F10.7=120

Tsunami: Uz=20m/s, Ux=±200m/s at surface

Uz=20m/s
Ux=±200m/s
Inclination = 30degree

vTEC

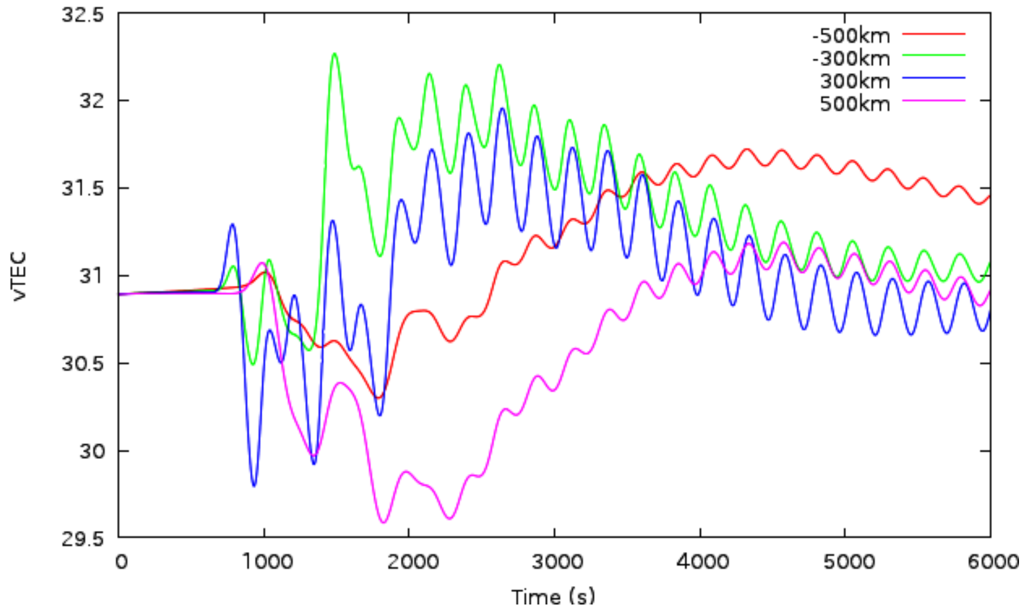

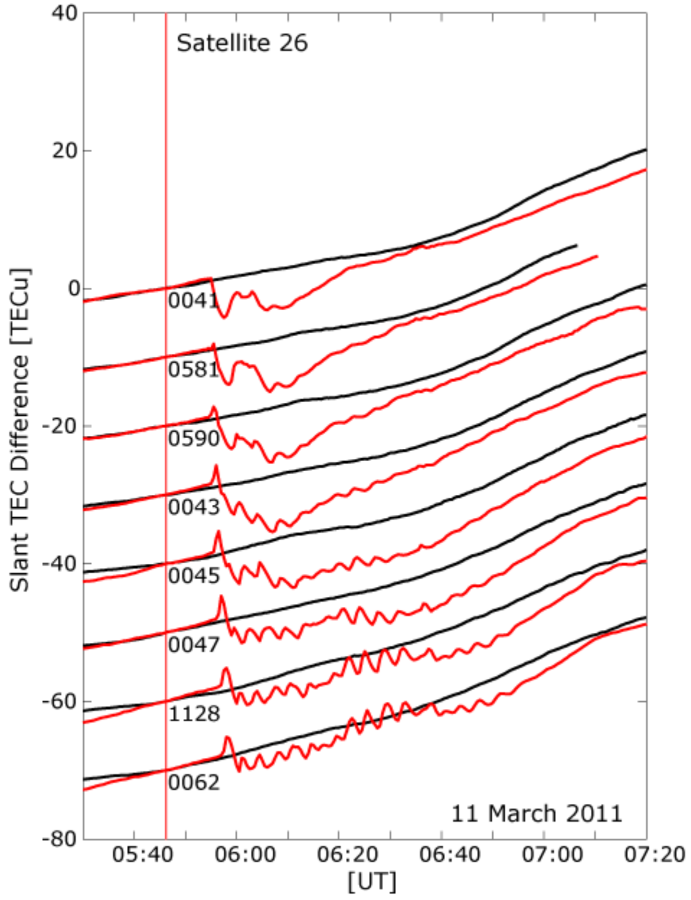

TEC enhancement at the beginning
TEC decrease during 1~2 hour
Small, Medium and Large scale TEC variations

1800 s

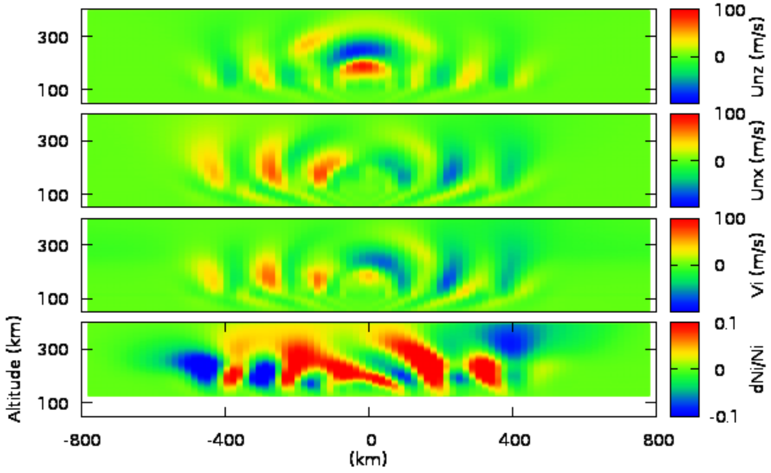

Inclination = 30degree
Ux=±200m/s
Uz=1m/s, T=600s
(Uz= sin(2π/T))
Inclination = 30degree

TEC Modeling

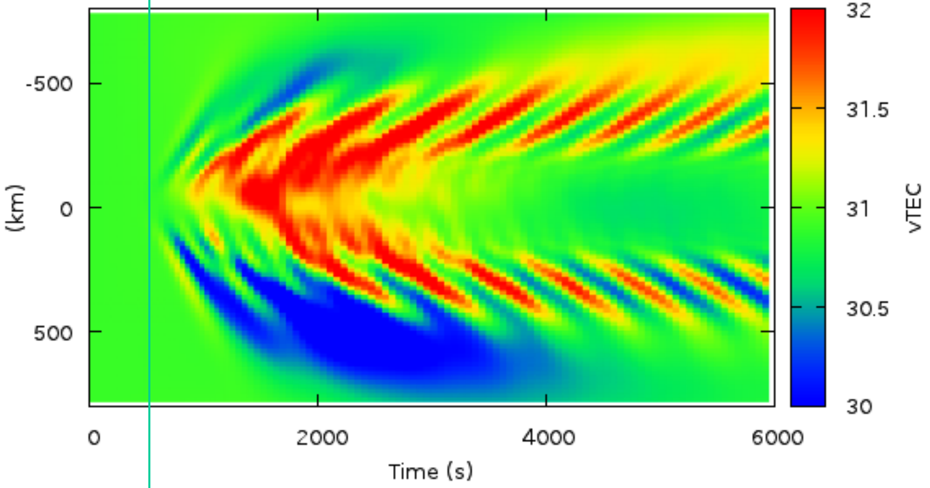

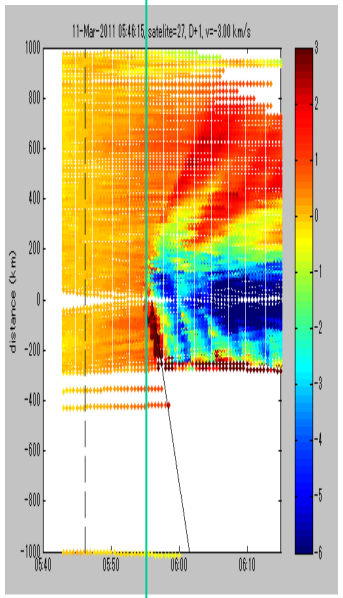

TEC by Satellite 26

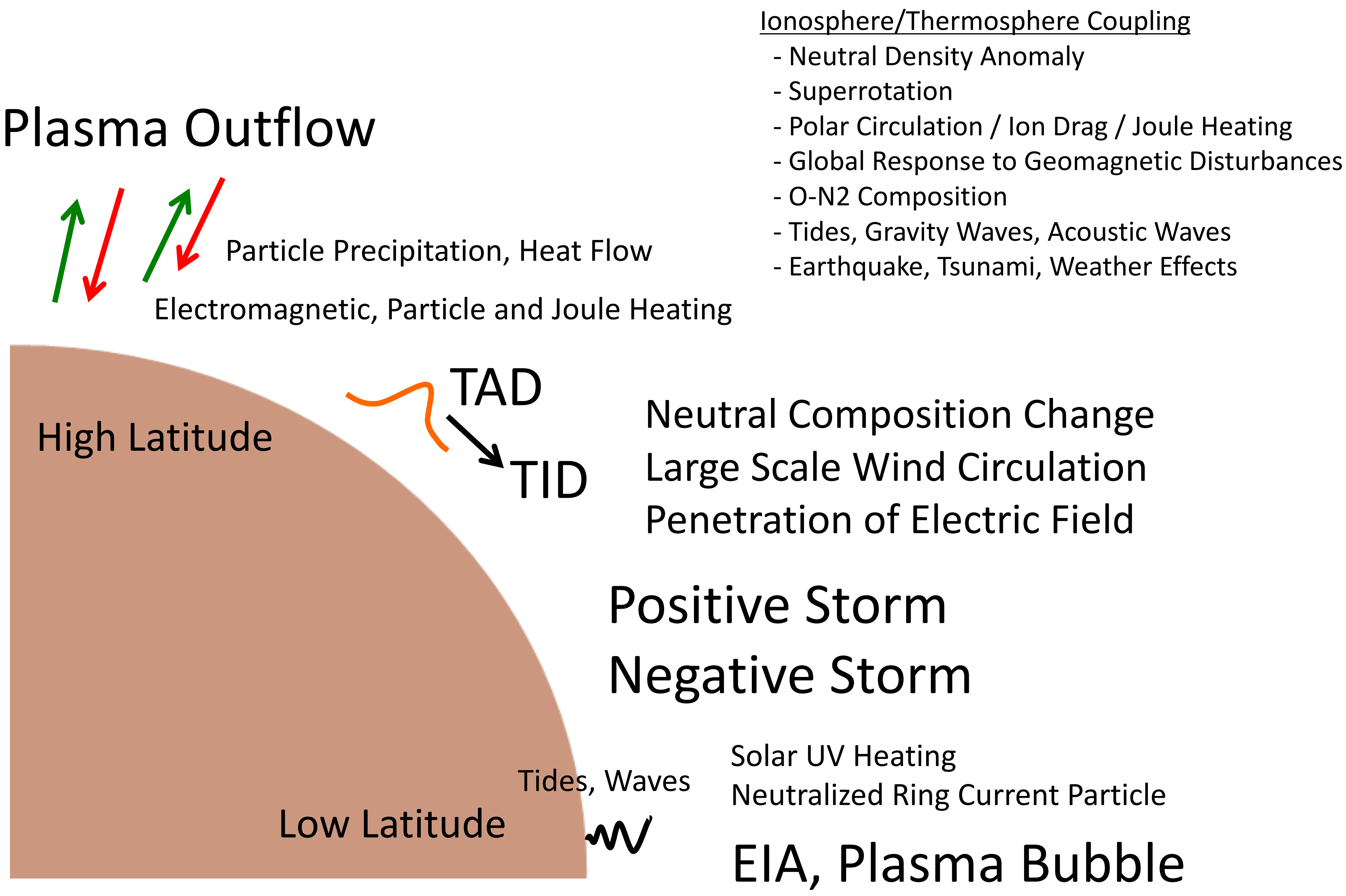
Ionosphere/Thermosphere Coupling
- Neutral Density Anomaly
- Superrotation
- Polar Circulation / Ion Drag / Joule Heating
- Global Response to Geomagnetic Disturbances
- O-N2 Composition
- Tides, Gravity Waves, Acoustic Waves
- Earthquake, Tsunami, Weather Effects
Plasma Outflow
Particle Precipitation, Heat Flow
Electromagnetic, Particle and Joule Heating
TAD
TID
High Latitude
Neutral Composition Change
Large Scale Wind Circulation
Penetration of Electric Field
Positive Storm
Negative Storm
Tides, Waves
Solar UV Heating
Neutralized Ring Current Particle
Low Latitude
EIA, Plasma Bubble

Please enjoy Space Science!